April 12, 2019

Dear editor,
We provide point-to-point reactions to your below given comments as well as an updated version of the manuscript.

Yours Sincerely,
Authors.

Editor comments on angeo-2018-93-manuscript-version7:

General comments

Impact of gradient mapping function (mfg): you show that using the BS mfg instead of the CH mfg makes a significant difference in the values of estimated gradients parameters (GE and GN) either by GNSS observations or from the NWM. This is indeed expected from the fact that the two MF's differ significantly at low elevations (e.g. the ratio CH/BS is 0.55 at 3 deg). This has several implications: 1) when comparing GNSS/CH and GNSS/BS variants to NWM/CH one can expect that agreement will be better for the GNSS/CH; 2) it is not possible to evaluate the absolute accuracy of GNSS gradients using NWM/CH gradients as they may contain a bias due to the particular mfg used to compute NWM/CH; 3) other approaches must be used if one wants to assess which mfg provides the more accurate GNSS gradient estimates. These remarks and warnings should be clearly stated in the manuscript (e.g. at end of Section 2). In a previous version of the manuscript you wrote that these comparisons should be treated cautiously (a sentence already revised). But I think the message should be much stronger.
Ad 1) we mention on this and warn the reader about the comparison of GNSS vs. NWM results in Section 3.3 – since we moved the previous section 3.3 to section 3.1, the numbering has changed! Ad 2) we now mention in the Conclusion section that the same mfg can be implemented in a different form which can also lead to biased results if tropospheric gradients from two sources are being compared and it is therefore important to check also how the particular mfg was implemented in the processing.
We think that the reader is now sufficiently aware of limitations of our study and of the selection of an appropriate gradient mapping function.

The results in Table 3 show that the mean difference GNSS/BS – ERA5 is the largest which is consistent with point 1). But the standard deviation (SD) of differences for GNSS/BS – ERA5 is the smallest which contradicts point 1). The explanation given by the authors is that NWM/CH provides smaller gradient estimates than GNSS which are in better agreement with the smaller GNSS/BS gradient estimates (i.e. by chance the biases are in the same direction). I agree with the explanation but this result doesn't add anything useful to the goal of the study. I think that this comparison should thus be removed from Table 3 to keep the flow of the discussion.
We decided to keep the GNSS/BS comparisons in the paper for the completeness. We think that we provide the reader enough information to be aware of the limitations of provided results.

Regarding point 3) inspection of position repeatability may help to assess the accuracy and compare the different processing variants (done in Section 3). You also discuss the results of another approach for the computation of gradients from the NWM gridded data based on the closed-form formulation of Davis et al. (1993). You report that this approach is in less good agreement with your GNSS/CH solution than your NWM/CH solution. Given the above remark this result was actually expected. Did you also compare the closed-form formulation results to your GNSS/BS solution? May it be that the agreement is higher? This comparison might actually help addressing points 2 and 3.

We do not understand "Given the above remark this result was actually expected". As stated in the manuscript, we think that the NWM tropospheric gradients obtained from the closed-form expression Davis et al. (1993) are in less good agreement with the GNSS tropospheric gradients, because the method to obtain NWM tropospheric gradients from a least square fit is closer to the method used with the GNSS. No, we did not compare the closed-form formulation results to our GNSS/BS solution. We do also not understand what you mean by point 3) above ("other approaches must be used if one wants to assess which mfg provides the more accurate GNSS gradient estimates"). What do you mean by "more accurate GNSS gradient estimates."? When we estimate tropospheric gradients by a least square fit (we can do this with the e.g. the GNSS, a NWM or a Water Vapor Radiometer) then, per definition, the tropospheric gradients depend on the gradient MF. We can define them utilizing the gradient MF by CH, but we can also define them by utilizing the gradient MF by BS. We cannot state that tropospheric gradients estimated with CH are more (or less) accurate than tropospheric gradients estimated with BS.

I was wondering how your gradient estimates compare to the gradient data provided by Tech. Univ. of Vienna. If I'm right their computation is based on the closed-form formulation. It would be very useful to the community if you can comment on the consistency of these various gradient data sources.

The comparison with data provided by TU Vienna is an excellent idea. Thank you for this suggestion. You are correct, the so-called LHGs (Linearized Horizontal Gradient) provided by TU Vienna are based on the closed-formulation, see Böhm et al. 2007. Recently, Landskron et al. 2018 provide refined horizontal gradients. They are based on a least square fit. They recommend using the refined horizontal gradients. It is clear that LHGs are of somewhat limited value. For example, TU Vienna recommends applying so called reduction factors. The LHG model is no longer supported. For details see http://vmf.geo.tuwien.ac.at/. Therefore, we decided to add in the manuscript a comparison of our NWM tropospheric gradients with the LHG and the refined horizontal gradients from TU Vienna (see end of Section 2.3 and mainly the Appendix B). The LHG model is only available for several stations. We decided to look at three stations available in all data sets: ONSA, POTS and WTZR. As to expect, we find a better agreement with the refined horizontal gradient model.

Added references:

Boehm, J. and Schuh, H.: Troposphere gradients from the ECMWF in VLBI analysis, Journal of Geodesy, 81, 403-408, doi: 10.1007/s00190-007-0144-2, 2007.

Landskron, D. and Boehm, J.: Refined discrete and empirical horizontal gradients in VLBI analysis, Journal of Geodesy, 92, 1387-1399, doi:10.1007/s00190-018-1127-1, 2018.

Zus, F., Douša, J., Dick, G., and Wickert, J.: Station specific NWM based tropo parameters for the Benchmark campaign, ES1206-GNSS4WEC COST Workshop, Iceland, 8–10 March 2016.

A have a final concern with Section 4. As I already expressed in the previous review and also pointed out by the two referees, the added value of Section 4 is rather poor. Though the impact of observation elevation-dependent weighting (OEW) is not negligible and should be carefully addressed, Section 4 provides only a qualitative assessment for one single day, and this assessment is based on 3 figures and 18 plots! What is the goal for each of the figures? Which additional conclusions are drawn from each of the figures? Which OEW scheme and mfg are recommended in the end? This section should be seriously revised and each of these questions should be addressed. Here are a few options for the presentation. Figure 5 could show only results for one OEW scheme and the results from the other variants could be described in the text since all the plots are actually very similar. Difference could be quantified in a Table. Figure 6: are all plots necessary? Maybe scatter plots would suffice to support the discussion and again the results from different variants

could be provided in a Table. Figure 7: what does the comparison of residuals add to the assessment of gradient estimates? Additional suggestions on Section 4 are given below in the specific comments.
Initially, we included only plots for two OEW schemes for gradients and differences. During the first review, we were asked why we haven't shown other weighting too. We then added them because a graphical visualization gives a clear view about behaviour of gradients (the size and orientation) at individual stations of the network showing patterns and impact due to both the gradient mapping function and the OEW scheme. The impact can be also study during events with significant gradients in a dense network only while it easily remains hidden in most other cases. That was our preference over a pure statistics or time series which can hardly show any details or overall behaviour.

In this context, we should also emphasize that our target was to estimate optimally tropospheric horizontal gradients during a severe weather event when the results could support numerical weather forecasting. Obviously, it doesn't necessarily have the same needs for estimation of gradients within the re-analysis. The reason is they are commonly included with a low temporal resolution and/or constrained for decorrelations. Then gradients are used mainly for improving the modelling of the troposphere for improving other parameters, mainly horizontal coordinates. So far in re-analysis, there were no aims at targeting optimal estimates of size and orientation of gradients.

Anyway, we fully revised Section 4.

Specific comments

Abstract:
"All solutions using final orbit and clock products provided tropospheric gradients with a clear relation to NWM outputs" what do you mean by a "clear relation to NWM outputs"?
We reformulated the sentence.

"The state-of-the-art models should be then applied for low-elevation observations for obtaining the best repeatability of the station coordinates" which state-of-the-art models are you referring to? Be more specific. I could not find any discussion on state-of-the-art models in the discussion of repeatability except "We also notice a slightly better performance in case of the BS mfg when compared to the CH mfg." Do you mean applying BS mfg? Or are you referring to the observation elevation-dependent weighting?
We reworded the whole sentence: "Comparisons of GNSS and NWM gradients suggest the 3° elevation angle cut-off and GPS+GLONASS constellation for obtaining optimal gradient estimates provided precise models for antenna phase centre offsets and variations and tropospheric mapping functions are applied for low-elevation observations."

"Although using simplified models..." which simplified models are you referring to? Do you suggest that the results are only preliminary and need be confirmed using more accurate models?
We removed the first part of the sentence – see above.

"Finally, systematic errors can affect the gradient components solely due to the use of different gradient mapping functions, and still depending on the applied observation elevation-dependent weighting. A latitudinal tilting of the troposphere in a global scale causes a systematic difference up to 0.3 mm in the north gradient component, while large local gradients, usually pointing to a direction of increasing humidity, can cause differences up to 0.9 mm in any component depending on the actual direction of the gradient." I have several concerns with this paragraph. I guess the 0.3 mm is referring to the Figure in the Appendix (though I don't get how the figure can be summarized in one single number when the map shows quite large latitudinal variation) and the 0.9 mm to another result from the main text (though I could not find surely it in any table or figure). The systematic errors which are mentioned seem to refer to the results of Section 4 (according to the title of this

section) but this section presents results from a single, so it is not possible to conclude on systematic errors.
We believe providing these numbers in abstract is relevant when these are purely referred to the extreme values – in both cases we thus used the words "can cause differences up to". Of course, an actual impact can be much smaller or even negligible, but we aimed at pointing to these potential differences which were commonly neglected in the community until today – either within gradient combinations, comparisons or interpretations.

From the global map (Appendix), maximum values can be clearly identified, and these are rather stable over time. For the regional maximum values, we identified the event with the most significant tropospheric gradients in order to demonstrate what can happen during a short period of up to several hours, i.e. in an actual situation when numerical weather forecasting can profit from accurate and high-resolution GNSS tropospheric horizontal gradients.

Please revise the Abstract including quantitative results from Section 3 to support your conclusions (e.g. systematic differences or errors are quantified in Table 2 and 3). Nothing is said about which gradient mapping function should be used.
We added a sentence regarding the gradient mapping function selection in the abstract. On the other hand, we prefer to keep the abstract in the current shape to keep it compact and easily understandable. The quantitative results are summarized in the Conclusion section.

Section 3: move the introductory text of this section (P7L26-P8L8) including Fig. 2 to a new subsection 2.4 "Comparison of gradient estimates". The general information belongs logically to the data and methods section as it informs about the data/station selection method, time sampling, and shows an illustration of time series which is actually not further analysed in Section 3 but is quite useful to get familiar with the magnitude of gradient parameters. This change implies very minor editing.
Section 2.4 was created.

This new sub-section should also be completed with the screening information that you mention in your answer to my previous comments. Especially, regarding the unrealistic cases with the RT3 solution, you write that some of them may not have been detected, and this is what I suspect from the bad results reported in Table 2 and 3 for RT3. I think the detection should be improved to remove all the unrealistic cases and statistics recomputed. This should not be difficult to implement given the specific features of these cases illustrated in Fig. 4 (e.g. compute an epoch-wise correlation coefficient of RT3 vs. ERA5 and detect the values below a fixed threshold).
Unrealistic cases with the RT3 solution were detected, the statistics were re-computed and updated in Table 2 and Table 3. Description of applied screening was added into the Section 2.4.

P7L12: "Results for individual… in Table 2" do you mean that the bias and SD in Table 2 are computed directly from the ZTD and gradient differences of all pairs of values (55 days x 243 stations x 288 estimates per day)? Another approach was followed by Dousa et al., 2016, 2017, who computed bias and SD of differences for each station and then statistics over the ensemble of stations. Please clarify which approach was used.
Yes, we used the first approach which you describe – statistics were computed directly from the ZTD and gradient differences of all pairs of values (55 days x 243 stations x 288 estimates per day).

P7L14: "standard deviation (SDEV) indicates a negligible impact" but later (P8L4-8) you conclude that all the differences are significant. Please be consistent.
The sentence was rewritten.

P7L16-17: "It should be noted that GLONASS observations were down-weighted by a factor of 1.5 in

dual-constellation variants of solution." This sentence should be moved in Section 2.2 and completed with an explanation (why did you down-weight GLONASS, what happens when one doesn't do it?).
We added the reasoning: "It should be noted that GLONASS observations were down-weighted by a factor of 1.5 in dual-constellation variants of solution to reflect both a lower quality of precise products and observations."

P7L21 to P8L4: Isn't it quite obvious that your GNSS comparisons will be more consistent than those in Dousa et al. 2016 (I guess you refer to Table 6 in this publication) who compared GNSS to NWM estimates where GNSS estimates were computed from different software? I suggest removing this paragraph. At least it is not useful for the analysis of your results in Table 2 which don't involve NWM results.
We removed this part of the text.

P8: The Wilcoxon signed-rank test is designed to test the null hypothesis that data come from a distribution whose median is zero. You write that "in all cases, the differences were found to be statistically significant". Are you sure about this? It is quite surprising that the null or very small ZTD biases (0.0 to 0.2 mm) and gradient biases (0.00 and +/- 0.01 mm) reported in Table 2 are significant. Please check.
We were also surprised by the results, however we checked them carefully and they are correct. To confirm them, we extra tested ZTD values from the pair GRCH3-GRBS3 in the IBM SPSS Statistics software and we got the same results. We provide graphical outputs from the SPSS testing here (solution1 = GRCH3, solution2 = GRBS3):

Hypothesis Test Summary

	Null Hypothesis	Test	Sig.	Decision
1	The distribution of solution1 is normal with mean 2,411.801 and standard deviation 39.538.	One-Sample Kolmogorov-Smirnov Test	.000	Reject the null hypothesis.
2	The distribution of solution2 is normal with mean 2,411.881 and standard deviation 39.586.	One-Sample Kolmogorov-Smirnov Test	.000	Reject the null hypothesis.

Asymptotic significances are displayed. The significance level is .05.

Hypothesis Test Summary

	Null Hypothesis	Test	Sig.	Decision
1	The median of differences between solution1 and solution2 equals 0.	Related-Samples Sign Test	,000	Reject the null hypothesis.
2	The median of differences between solution1 and solution2 equals 0.	Related-Samples Wilcoxon Signed Rank Test	,000	Reject the null hypothesis.
3	The distributions of solution1 and solution2 are the same.	Related-Samples Friedman's Two-Way Analysis of Variance by Ranks	,000	Reject the null hypothesis.
4	The distributions of solution1 and solution2 are the same.	Related-Samples Kendall's Coefficient of Concordance	,000	Reject the null hypothesis.

Asymptotic significances are displayed. The significance level is ,05.

P8L6: provide a reference to the Wilcoxon signed-rank test
Reference added: https://docs.scipy.org/doc/scipy/reference/generated/scipy.stats.wilcoxon.html.

P7-P8: please review and revise your comments on results from Table 2. They would gain in legibility if you discuss ZTD first and then gradients, and proceed in the order bias, SD, and CC, and row by row. Especially, the impact of changing the mfg on the bias is noticeable and consistent with what is expected from Fig. 1. So at least it would be good to start with this one.
Whole text discussing results from Table 2 was edited in order to increase its legibility. Although we do not discuss firstly ZTD and then gradients as you suggested, we keep the order of the parameters – mean difference, SD, CC.

Table 2: update signs in gradient mean differences (due to reversal of differences RT* - GxCH3 from previous version of the manuscript)
Corrected, thank you for notification.

P10: significance of biases reported in Table 3: again check the results because it is suspicious that the small values are significant.
We checked the results, they are correct.

P9-11: please review and revise your comments on results from Table 3.
We slightly edited the text describing results given in Table 3.

P11L6-10: I suggest that you remove the comparison between GNSS/BS and NWMs.
We decided to keep them in the paper for completeness.

Section 3.3: this sub-section would be usefully moved at the head of section 3 as it introduces the overall characteristics of the data set and provides a first intercomparison of the impact of the various processing options and the consistency with the NWMs. This knowledge would then help in

the interpretation and discussion of the results from Table 2 and 3, namely regarding the significance of the results (mean and SD of difference of gradients are very small < 1 mm). The title could be changed to "Comparison of mean gradients and formal errors).
We moved this sub-section to the beginning of Section 3.

P15L2-3: "This discrepancy might be attributed to a slightly worse modelling of low-elevation observations when using the GPT+GMF" can you provide a reference to this?
Douša et al. (2017) indicated also worse results when using GPT+GMF compared to VMF1 which can be attributed to modelling errors in the former particularly if applied in PPP (Kouba 2009).

Douša, J., Václavovic, P. and Eliaš, M.: Tropospheric products of the second European GNSS reprocessing (1996-2014), Atmospheric Measurement Techniques, 10, 3589–3607, doi:10.5194/amt-10-3589-2017, 2017.

Kouba, J.: Testing of global pressure/temperature (GPT) model and global mapping function (GMF) in GPS analyses, Journal of Geodesy, 83, 199–208, doi:10.1007/s00190-008-0229-6, 2009.

P15L4-5: "We also notice a slightly better performance in case of the BS mfg when compared to the CH mfg." Please apply the statistical test to check whether the difference is significant or not. This might have a strong implication on the conclusions since position repeatability can be regarded as an objective criterion for the assessment of the accuracy of the GNSS solution and help to select the optimal processing variant.
We firstly tested the normality of coordinates repeatability in all three components for GRCH3 and GRBS3 solutions and found out that they do not follow a normal distribution. Therefore, we applied the Wilcoxon signed-rank test and according to its results the difference is statistically significant in North and Up component at the 5% significance level. We added this information to the manuscript.

P15L8-9: "lower quality of the IGS03 RT product during some periods, see Figure 4." Again, the results should not be corrupted by outliers as this prevents from assessing the real accuracy of the RT3 solution. Please compute again these statistics after removing the erroneous cases.
Tropospheric gradients were during the GNSS data processing estimated epoch-wisely while the coordinates were estimated on a daily basis. Since epochs with unrealistic tropospheric gradients in the RT3GxCH3 solution were identified in 28 days, we would have to exclude these 28 days from the coordinates repeatability computation. Due to this reason we keep the original results in the paper.

On the other hand, we re-computed all other results in tables 4 and 5 (formal errors of tropospheric gradients, mean gradient angles and magnitudes) and updated the manuscript accordingly.

Section 4: the title is not reflecting the content. I suggest to change to: "Additional assessment of processing options".
Changed to: "Systematic effects induced by gradient mapping functions and elevation-dependent weighting"

P16L9-10: "Magnitudes of individually estimated gradients from nearby stations show better consistency…" you suggest that a more homogeneous gradient field is of better quality? Why?
Considering the gradients estimated in PPP are not affected by the errors stemming from the precise products, these should reflect actual weather conditions. Fortunately, the PPP is stand-alone method (data processed independently at each station), thus gradients estimated from two nearby stations should reflect similar conditions and thus similar values can be considered highly realistic. And even in opposite way, the gradients should not indicate significantly different magnitudes or directions for such stations or within local variabilities or patterns in a dense network.

Results from Figure 5: it is not possible to decide if one of the 8 displayed gradient maps is more accurate/realistic without comparing them to a reference map and/or using an objective metrics (RMSE, etc). You can only comment on the differences and the impact of OEW and mfg settings.
We agree, but we haven't tried this. However, as we fully revised the section, we believe there is no any such statement.

P18L2-5: "Such differences depend on both the magnitude and direction of estimated gradients when these are decomposed into two components. In our case, positive differences in north and east component appear when the estimated gradients point to south and west, respectively, and negative differences occur when the gradients point to opposite directions." => this sentence could be clarified as "We have seen previously that the magnitude of CH gradients is larger compared to BS gradients. The sign of the gradient differences depends thus on the direction (north/south for GN and east/west for GE) of the CH gradients, i.e. positive differences in north and east component appear when the estimated gradients point to south and west, respectively, and negative differences occur when the gradients point to opposite directions". However, in this reasoning it is assumed that for any given pair of gradients, the magnitude of CH gradients is larger than that of BS gradients. This is not demonstrated (Fig. 1 shows the overall distribution but not the point by point relationship). Hence, a scatterplot of BS gradient vs. CH gradient should be rather shown.
The sentence was clarified as suggested. The higher magnitudes of CH gradients were clearly visible in Figure 5 (now in Figure 6) and it was discussed in Section 2.2 as it is a product of the gradient term in Eq. 1.
We do believe it does not need a scatter plot (thought we added them), which does not give clearer picture.

P20L1-4: "The SINEL2 OEW scheme in the left panel shows more homogenous distribution of carrierphase post-fit residuals above the elevation angle of 30° when compared to the EQUAL scheme (right panel) …" => this is not what is seen in the Figure: the EQUAL residuals are more homogeneous while the SINEL2 residuals vary roughly as 1/sin2(e) as one can expect from the applied OEW scheme. I don't think this figure adds something to the analysis of the gradient modelling schemes.
The paragraph was fully reworded. Anyway, we assessed the homogeneity of post-fit residuals mainly for high elevations (above 30deg at least) and close to the zenith, where any contributing errors should be the smallest.

Conclusions

P20L25: reference to (Guerova et al., 2016)
Guerova, G., Jones, J., Dousa, J., Dick, G., de Haan, S., Pottiaux, E., Bock, O., Pacione, R., Elgered, G., Vedel, H., and Bender, M.: Review of the state-of-the-art and future prospects of the ground-based GNSS meteorology, Atmos. Meas. Tech., 9, 5385-5406, 2016
Reference added.

P21L28-29: "It affects the gradient magnitudes, not their directions, however, the gradient direction results in different projections into gradient components." Awkward sentence. Please revise.
Reworded: "While the mfg choice affects the magnitude of estimated gradient, it does not affect the direction of the gradient. However, any difference in the magnitude causes systematic errors in gradient components which depend on the gradient direction too."

Syntax
Replace all PP acronyms with post-processing (only a few times in the document)
Done.

Replace all SDEV acronyms with SD
Done.

Sensitivity of GNSS tropospheric gradients to processing options

Michal Kačmařík[1], Jan Douša[2], Florian Zus[3], Pavel Václavovic[2], Kyriakos Balidakis[3], Galina Dick[3], Jens Wickert[3,4]

[1] Department of Geoinformatics, VŠB – Technical University of Ostrava, Ostrava, The Czech Republic
[2] Geodetic Observatory Pecný, Research Institute of Geodesy, Topography and Cartography, Zdiby, The Czech Republic
[3] GFZ German Research Centre for Geosciences, Potsdam, Germany
[4] Institute of Geodesy and Geoinformation Science, Technical University of Berlin, Germany

Correspondence to: M. Kačmařík (michal.kacmarik@vsb.cz)

Abstract. An analysis of processing settings impact on estimated tropospheric gradients is presented. The study is based on the benchmark data set collected within the COST GNSS4SWEC action with observations from 430 GNSS reference stations in central Europe for May and June 2013. Tropospheric gradients were estimated in eight different variants of GNSS data processing using Precise Point Positioning (PPP) with the G-Nut/Tefnut software. The impact of the gradient mapping function, elevation cut-off angle, GNSS constellation, observation elevation-dependent weighting and real-time versus post-processing mode were assessed by comparing the variants by each to other and by evaluating them with respect to tropospheric gradients derived from two numerical weather prediction models (NWM). Tropospheric gradients estimated in post-processing GNSS solutions using final products were in a good agreement with NWM outputs. ~~All solutions using final orbit and clock products provided tropospheric gradients with a clear relation to NWM outputs.~~ ~~However, the~~The quality of high-resolution gradients estimated in (near) real-time PPP analysis still remains challenging task due to the quality of the real-time orbit and clock corrections. ~~Although using simplified models, the c~~Comparisons of GNSS and NWM gradients suggest~~s~~ the 3° elevation angle cut-off and GPS+GLONASS constellation for obtaining optimal gradient estimates provided. ~~The state-of-the-art~~ precise models for antenna phase centre offsets and variations and tropospheric mapping functions ~~should be then~~are applied for low-elevation observations ~~for obtaining the best repeatability of the station coordinates~~. Finally, systematic errors can affect the gradient components solely due to the use of different gradient mapping functions, and still depending on ~~the applied~~ observation elevation-dependent weighting. A latitudinal tilting of the troposphere in a global scale causes a systematic difference up to 0.3 mm in the north gradient component, while large local gradients, usually pointing to a direction of increasing humidity, can cause differences up to ~~0.9~~1.0 mm (or even more in extreme cases) in any component depending on the actual direction of the gradient. Although the Bar-Sever gradient mapping function provided slightly better results in some aspects, it is not possible to give any strong recommendation on the gradient mapping function selection.

1 Introduction

When processing data from Global Navigation Satellite Systems (GNSS), a total signal delay due to the troposphere is modelled by epoch- and station-wise Zenith Total Delay (ZTD) parameters, and, optimally, together with tropospheric gradients representing the first order asymmetry of the total delay. ZTDs, which are closely related to Integrated Water Vapour (IWV), are operationally assimilated into Numerical Weather Prediction models (NWM) and have been proven to improve precipitation forecasts (Vedel and Huang, 2004, Guerova et al., 2006, Shoji et al., 2009). Previous studies demonstrated that the estimation of tropospheric gradients improves GNSS data processing mainly in terms of receiver position and ZTDs (Chen and Herring, 1997, Bar-Sever et al., 1998, Rothacher and Beutler, 1998, Iwabuchi et al., 2003, Meindl et al., 2004). Nowadays, tropospheric gradients are not assimilated into NWMs, however, they could be assimilated in future (see Zus et al., 2019) and they are essential for reconstructing slant total delays (STD). The STDs represent the signal travel time delay between the satellite and the station due to neutral atmosphere and they are considered useful in numerical weather prediction (Järvinen et al., 2007, Kawabata et al., 2013, Bender et al., 2016) and reconstruction of 3D water vapor fields using the GNSS tomography method (Flores et al., 2000, Bender et al., 2011).

Brenot et al. (2013) showed a significant improvement of IWV interpolated 2D fields when tropospheric gradients are taken into account. With the improved IWV fields, the authors studied small scale tropospheric features related to thunderstorms. Douša et al. (2018a) demonstrated the advantage of using tropospheric gradients in the 2-stage troposphere model combining NWM and GNSS data. Morel et al. (2015) presented a comparison study on zenith delays and tropospheric gradients from 13 stations at Corsica Island in the year 2011. Despite a good agreement in the ZTD, they found notable discrepancies in tropospheric gradients when estimated by using two different GNSS processing software, two different gradient mapping functions, and two different processing methods: 1) double-differenced network solution, and 2) Precise Point Positioning, PPP (Zumberge et al., 1997) solution. Douša et al. (2017) indicated a problem with systematic errors in tropospheric gradients due to absorbing instrumentation errors. Few attempts were made to compare the tropospheric gradients with independent estimates, i.e., those derived from Water Vapor Radiometer (WVR) or NWM data. For a selected number of stations such a comparison was made in Walpersdorf et al. (2001) where ZTDs and tropospheric gradients from GPS were compared with those derived from a high-resolution NWM ALADIN. A good correlation between GPS and NWM gradients was found for inland stations, but not for coastal ones. More recently Li et al. (2015) and Lu et al. (2016) showed that with the upcoming finalization of new systems such as Galileo and BeiDou the improved observation geometry yields more robust tropospheric gradient estimates. Li et al. (2015) found an improvement of about 20~35% for the multi-GNSS processing when compared with NWM and 21~28% when compared to WVR. Another multi-GNSS study on tropospheric gradients (Zhou et al., 2017) used data from a global network of 134 GNSS stations processed in six different constellation combinations in July 2016. An impact of gradients estimation interval (from 1 to 24 h) and cut-off elevation angle (between 3° and 20°) on a repeatability of receiver coordinates was examined. Better results were found for solutions where a shorter time interval of tropospheric gradient estimation was used and where the elevation cut-off angle of 7° or 10° was applied. However, strategies were not

compared from the point of view of actually obtained gradient values. Finally, systematic differences and impacts of a gradient mapping function or observation elevation weighting on estimated gradients have not been studied yet.

In this work, we systematically evaluate the quality of tropospheric gradients estimated from a regional GNSS dense network under different atmospheric conditions. Using a unique data set, we study the impact of several approaches. ZTDs and tropospheric gradients are then compared with the ones estimated from two NWMs – ERA5, which is a global atmospheric reanalysis, and a limited area short range forecast utilizing the Weather Research and Forecasting (WRF) model. Finally, we quantified systematic differences in tropospheric gradients coming from the gradient mapping function and the method of observation weighting during a local event with strong wet gradients.

2 Data and Methods

2.1 Benchmark data set

The benchmark campaign was realized within the European COST Action ES1206 GNSS4SWEC to support development and validation of a variety of GNSS tropospheric products. An area in central Europe covering Germany, the Czech Republic and part of Poland and Austria was selected as a domain while May and June 2013 as a suitable time period due to occurrence of severe weather events including extensive floods. Data from 430 GNSS stations were collected together with meteorological observations from various instruments (synoptic, radiosonde, WVR, meteorological radar, etc.). In addition, tropospheric parameters from two global and one regional NWMs were generated. Detailed information about the benchmark campaign can be found in Douša et al. (2016). Although the presented study is based on the GNSS data collected within the benchmark campaign, all the presented GNSS and NWM solutions were newly prepared for this study.

2.2 Estimation of tropospheric gradients from GNSS

The STD as a function of the azimuth (a) and elevation (e) angle can be written as follows:

$$STD(a,e) = mfh(e) * ZHD + mfw(e) * ZWD + mfg(e) * (Gn * cos(a) + Ge * sin(a)) \quad (1)$$

where ZHD denotes the Zenith Hydrostatic Delay and ZWD denotes the Zenith Wet Delay. The elevation angle dependency is given by mapping functions, which are different for the hydrostatic (*mfh*), wet (*mfw*) and gradient (*mfg*) part. The tropospheric horizontal gradient vector is defined in the local horizontal plane with two components, one for the north-south direction (*Gn*) and one for the east-west direction (*Ge*). From the formula (1) is evident that GNSS gradient represents a gradient of both hydrostatic and wet part of the delay, therefore a total delay gradient.

During GNSS data processing, the ZHD is commonly taken from an a priori model, e.g. Saastamoinen (1972) or Global Pressure and Temperature (GPT, Boehm et al., 2007a) based on climatological data, or it can be derived from NWM data. The ZWD, or a correction to the modelled ZHD, and tropospheric gradients are estimated as unknown parameters using a deterministic or stochastic model.

Current mapping functions for hydrostatic (*mfh*) and wet (*mfw*) delay components are based either on climatological data, e.g. Global Mapping Function, GMF (Boehm et al., 2006a) or NWM data, e.g. Vienna Mapping Function, VMF (Boehm et al., 2006b). An advantage of the first approach is its independence of external data. Several mapping functions for tropospheric gradients have also been developed in the past, e.g. by Bar-Sever et al. (1998), by Chen and Herring (1997), or the tilting mapping function introduced by Meindl et al. (2004). The gradient mapping function (*mfg*) by Bar-Sever (BS) is given as

$$mfg = mfw * cot(e) \quad (2)$$

and from the formula is apparent that it depends on the selected *mfw*. The Chen and Herring (CH) *mfg* reads as

$$mfg = 1 / (sin(e) * tan(e) + c) \quad (3)$$

where $c = 0.0032$. Since c is related to the scale height, it experiences spatiotemporal variations. Nevertheless, based on Balidakis et al. (2018) a variable c does not yield a statistically significant improvement in describing the atmospheric state over a constant c. Finally, the tilting mapping function is defined in a generic way as a ~~tilting~~ derivative of the *mfw* ~~by using the so-called tropospheric zenith z and can be expressed as~~with respect to the elevation angle

$$mfg = -\partial(mfw)/\partial ~~z~~e \quad (4)$$

Figure 1 illustrates the variability of the gradient contribution term ($Gn * cos(a) + Ge * sin(a)$) in Eq. (1) and the size of the mapping factors represented by actual values of the three *mfg*. We included gradient contributions corresponding to all GNSS observations in the benchmark campaign during a single day (May 31, 2013). Obviously, an actual magnitude of the gradient depends on the mapping factor. While the BS *mfg* generates ~~the highest~~ higher mapping factors and thus smaller gradient contributions term (scatters in y-axis), the CH *mfg* provides ~~the lowest~~ lower mapping factors and~~, consequently,~~ thus higher gradient ~~values~~contribution terms. The tilting *mfg* gives then factors in between BS and CH *mfg* and results in gradient contributions in between the two. We can thus further focus on BS and CH *mfg* only as these can be considered as two extreme cases.

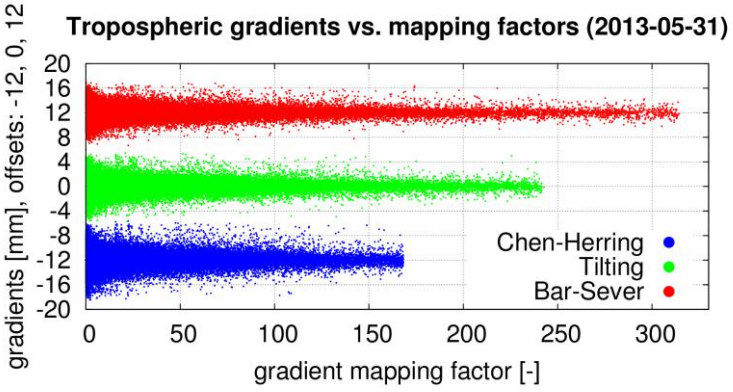

Figure 1. Variability of gradient mapping factors and tropospheric gradient contributions expressed in azimuths of individual satellites. Three *mfg* were studied on May 31, 2013: Chen and Herring *mfg* (blue), Bar-Sever *mfg* (red) and tilting *mfg* (green).

We use the G-Nut/Tefnut software (Václavovic et al., 2014) for GNSS data processing of the benchmark campaign. This software utilizes the PPP method and is capable of multi-GNSS processing in real-time (RT), near-real time (NRT) and post-processing (PP) mode with a focus on all the tropospheric parameters estimation: ZTDs, tropospheric gradients and slant delays (Douša et al., 2018b). Stochastic modelling of the troposphere allows an epoch-wise parameter estimation by extended Kalman filter in RT solutions (FLT) or its combination with a backward smoother which is used for NRT and ~~PP~~ post-processing solutions (FLT+SMT), see Václavovic and Douša (2015).

Table 1 describes all eight variants of solution for the benchmark campaign produced using the G-Nut/Tefnut which differ in (a) elevation cut-off angle (3° or 7°), (b) gradient mapping function (Chen and Herring = CH or Bar-Sever = BS), (c) constellations (GPS only = Gx or GPS+GLONASS = GR) and (d) processing mode (post-processing using the FLT+SMT processing or simulated real-time using the FLT processing only). Five variants based on the post-processing mode used the backward smoother and the ESA final orbit and clock products (http://navigation-office.esa.int/GNSS_based_products.html). Three variants, abbreviated as RT1GxCH3, RT3GxCH3 and RTEGxCH3, were used to test the performance of the Kalman filter and RT orbit and clock corrections using the IGS01 (RT1GxCH3) and IGS03 (RT3GxCH3) corrections from the IGS Real-Time Service (RTS, http://rts.igs.org). The IGS01 RTS product is a GPS only single-epoch solution produced using software developed by ESA/ESOC. The IGS03 product is a GPS+GLONASS solution based on the Kalman filter and the BKG's BNC software. The last solution, RTEGxCH3, applying the ESA final product is used to test a benefit of the backward smoothing on the one hand, and, an impact of the quality of RT corrections on the other hand. Unfortunately, the solution based on the processing of GPS+GLONASS data in the simulated RT mode had to be rejected due to a highly variable quality of RT corrections in 2013 affecting mainly the GLONASS contribution (and we noted temporal problems in GPS solutions too, see Figure 4).

The GPT model was used for calculating a priori ZHDs and the GMF was used for mapping hydrostatic and wet delays to the zenith. Estimated tropospheric parameters are thus independent from any meteorological information. GNSS observations were processed using 30-hour data batches when starting six hours before the midnight of a given day in order to eliminate the PPP convergence. In all variants, the observation sampling of 300 s was used with ZTDs and tropospheric gradients estimated for every epoch. The station coordinates were estimated on a daily basis. The random walk of 6 mm/sqrt(hour) was applied for the ZTD and 1.5 mm/sqrt(hour) for the gradients. Absolute IGS model IGS08.ATX was used for the antenna phase centre offsets and variations. All variants used the elevation observation weighting of $1/sin^2(e)$.

Table 1. Processing parameters of individual variants from the G-Nut/Tefnut software. Mode FLT denotes to simulated real-time solution using Kalman filter only, FLT+SMT to post-processing solution using the Kalman filter and the backward smoother.

Solution name	Elevation cut-off	Constellation	Gradient mapping function	Products	Mode
GxCH3	3	GPS	Chen and Herring	ESA final	FLT+SMT
GRCH3	3	GPS+GLONASS	Chen and Herring	ESA final	FLT+SMT
GRBS3	3	GPS+GLONASS	Bar-Sever	ESA final	FLT+SMT

GxCH7	7	GPS	Chen and Herring	ESA final	FLT+SMT
GRCH7	7	GPS+GLONASS	Chen and Herring	ESA final	FLT+SMT
RT1GxCH3	3	GPS	Chen and Herring	IGS01 RT	FLT
RT3GxCH3	3	GPS	Chen and Herring	IGS03 RT	FLT
RTEGxCH3	3	GPS	Chen and Herring	ESA final	FLT

2.3 Estimation of tropospheric gradients from NWM

Tropospheric gradients and zenith delays were derived from the output of two different numerical weather models; the ERA5 (https://www.ecmwf.int/en/forecasts/datasets/archive-datasets/reanalysis-datasets/era5) and a simulation utilizing the Weather Research and Forecasting (WRF) model (Skamarock et al., 2008). The ERA5 is a reanalysis produced at the European Centre for Medium-Range Weather Forecasts (ECMWF). The pressure, temperature and specific humidity fields are provided with a horizontal resolution of approximately 31 km (T639 spectral triangular truncation) on 137 vertical model levels (up to 0.01 hPa) every hour. The WRF simulations are performed at GFZ Potsdam. The initial and boundary conditions for the limited area 24-hour free forecasts (starting every day at 0 UTC) stem from the analysis of the Global Forecast System (GFS) of the National Centers for Environmental Prediction (NCEP). The pressure, temperature and specific humidity fields are available every hour with a horizontal resolution of 10 km on 49 vertical model levels (up to 50 hPa).

The ray-trace algorithm by Zus et al. (2012) is used to compute STDs. The tropospheric gradients are derived from STDs as follows. At first, 120 STDs are computed at elevation angles 3°, 5°, 7°, 10°, 15°, 20°, 30°, 50°, 70°, 90° and all azimuths between 0° and 360° with an interval of 30°). Second, we compute azimuth-independent STDs from the local vertical refractivity profile. Third, the differences between the azimuth-dependent STDs and the azimuth-independent STDs are computed. Finally, the gradient components are determined by a least-square fitting. For details the reader is referred to the Appendix in Zus et al. (2015).

Using ten years of ERA5 ~~long term~~ global data, we tested different observation elevation weighting schemes (equal versus the elevation dependent weighting of $1/\sin^2(e)$) and two *mfg*s (BS and CH) in the least squares parameter fitting. While using different observation elevation weighting schemes led to negligible differences in the tropospheric gradients, we found a significant systematic difference in the north gradient component between tropospheric gradients derived with BS and CH *mfg* (see Appendix A). In this regard it is important to note that NWM derived tropospheric gradients presented in this study were computed using CH *mfg*.

We ~~also~~ note that tropospheric gradients can be ~~derived (approximated)~~computed with the closed form expression depending on the north-south and east-west horizontal gradient of refractivity (Davis et al., 1993). We compared the ERA5 tropospheric gradients derived with our method and the closed-form method ~~the two different methods~~ with GNSS tropospheric gradients~~. We utilized the ERA5 and GNSS~~from the GRCH3 ~~data~~solution. We find that for the considered stations (over the entire benchmark period) the root-mean square deviation between NWM and GNSS tropospheric gradients is 10 % smaller if we apply ~~the first~~our method instead of the ~~second~~ closed-form method. This can be explained by the fact that ~~the first approach,~~

~~that is, calculating tropospheric gradients from ray-traced delays by least square adjustment, is the approach which~~our method is closer to the method actually applied in the GNSS analysis (parameter estimation).

We also compared our NWM tropospheric gradients with NWM tropospheric gradients provided by the TU Vienna (see Appendix B). We found a good agreement between the estimates, in particular between our tropospheric gradients and the so called refined horizontal gradients (Landskron and Boehm, 2018).

2.4 Comparison of gradient estimates

Absolute values of tropospheric gradient components stay typically below 1-2 mm under standard atmospheric conditions and can reach 4-6 mm during severe weather conditions. The gradient of 1 (6) mm corresponds to about 55 (330) mm slant delay correction when projected to 7° elevation angle. For an illustration an example time series of tropospheric gradients at station LDB2 (Brandenburg, Germany) for a period between May 15 and June 15, 2013 is given in Figure 2.

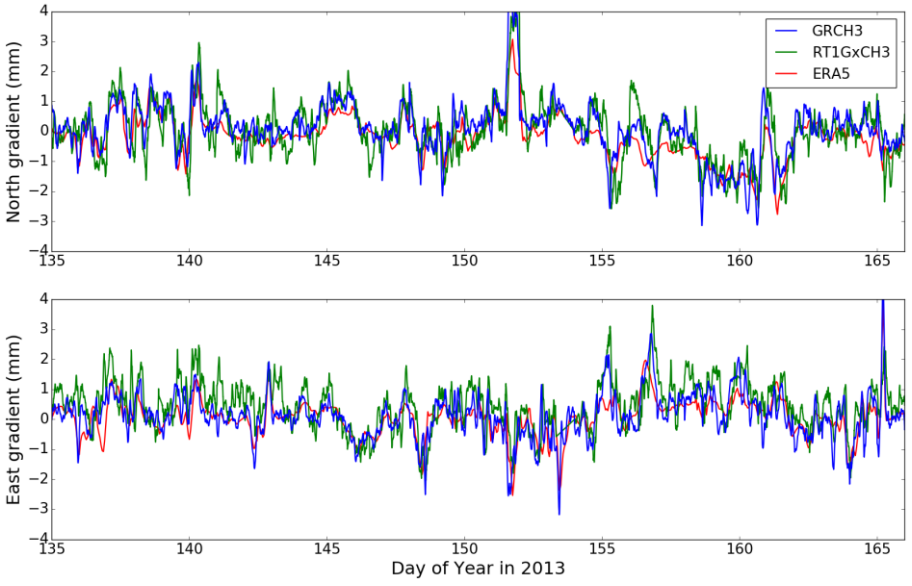

Figure 2. Tropospheric gradients retrieved from GNSS data processing (GRCH3, RT1GxCH3) and from NWM ERA5 at station LDB2 (52.209°N, 14.121°E, Germany) for a period from May 15, 2013 till June 15, 2013.

In the presented study, ZTDs and tropospheric gradients from all eight GNSS variants were compared to each other and also to the tropospheric parameters from ERA5 and WRF to evaluate the impact of various settings in GNSS data processing. Although about 430 GNSS stations are available in the benchmark data set, statistical results given in ~~this~~the ~~s~~Section 3 are based on a subset of 243 stations. Firstly, 84 stations without the capability of receiving GLONASS signals were excluded. Secondly, stations which did not have at least 5 % of all the observations in the range of elevation angles between 3° and 7° were excluded as well. This rule was applied to allow a systematic evaluation of elevation cut-off angle impact on tropospheric parameters. The majority of the stations (103) had to be excluded because of inability to provide a sufficient number of observations at very low elevation angles. During the statistics computation a standard data screening was applied to exclude

outlier values. Moreover, epochs were RT GNSS variant of solution RT3GxCH3 provided unrealistic tropospheric gradients (see Section 3.3) were also excluded from all the statistics computation except from the coordinates repeatability evaluation. Tropospheric parameters from the G-Nut/Tefnut software were provided every 5 minutes while the output from both NWM models was available every hour. Therefore, comparisons between GNSS solutions (Section 3.2) are based on a 5-minute interval while comparisons between GNSS and NWM solutions (Section 3.3) are based on a 1-hour interval.

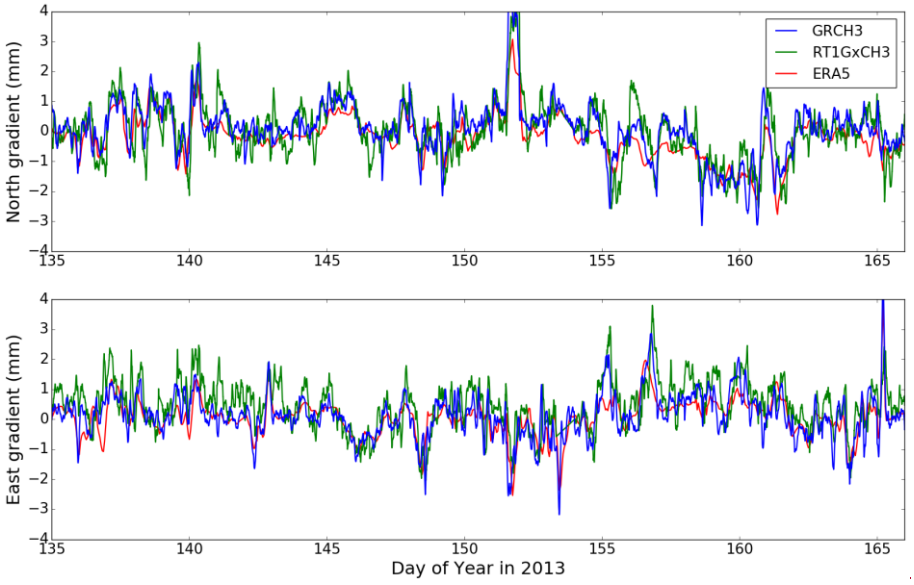

Figure 2. Tropospheric gradients retrieved from GNSS data processing (GRCH3, RT1GxCH3) and from NWM ERA5 at station LDB2 (52.209°N, 14.121°E, Germany) for a period from May 15, 2013 till June 15, 2013.

3 Impact of applied processing settings on GNSS tropospheric gradients estimation

ZTDs and tropospheric gradients from all eight variants were compared to each other and to the tropospheric parameters from ERA5 and WRF to evaluate the impact of various settings in GNSS data processing. Although about 430 GNSS stations are available in the benchmark data set, statistical results given in this section 3 are based on a subset of 243 stations. Firstly, 84 stations without the capability of receiving GLONASS signals were excluded. Secondly, stations which did not have at least 5 % of all the observations in the range of elevation angles between 3° and 7° were excluded as well. This rule was applied to allow a systematic evaluation of elevation cut-off angle impact on tropospheric parameters. The majority of the stations (103) had to be excluded because of inability to provide a sufficient number of observations at very low elevation angles.

Tropospheric parameters from the G-Nut/Tefnut software were provided every 5 minutes while the output from both NWM models was available every hour. Therefore, comparisons between GNSS solutions are based on a 5-minute interval while comparisons between GNSS and NWM solutions are based on a 1-hour interval.

The section starts with an introductory evaluation of mean tropospheric gradients and formal errors of their estimates. This is followed by comparisons between individual GNSS solutions and comparisons between GNSS and NWM solutions.

3.1 Comparison of mean tropospheric gradients and formal errors of their estimates

Mean gradient magnitudes and azimuth angles (direction of gradient) over the whole benchmark period were computed for 243 GNSS stations and are presented in Table 2. Mean magnitudes of tropospheric gradients from all post-processing GNSS variants oscillated around 0.85 mm and 0.67 mm when using the CH *mfg* and the BS *mfg*, respectively. The latter shows about 17 % smaller gradients compared to the former if all the processing aspects remained identical. Both RT solutions also resulted with higher gradient magnitudes, namely +14 % for RT1GxCH3 and +42 % for RT3GxCH3 when compared to the corresponding GxCH3 post-processing variant. A mean gradient magnitude of about 0.7 mm was found for both NWM solutions, i.e. of about 0.1 mm smaller than for the GRCH3 solution. This can be mainly explained by the limited horizontal resolution of the NWMs.

Table 2 shows that mean tropospheric gradients point towards the equator what is in an agreement with Meindl et al. (2004). Such a mean gradient direction does not depend on the gradient mapping function. By adding GLONASS observations the mean gradient direction was changed by +2°, however, actual effects were found to be highly station-dependent with a typical range of ±5° for individual stations. The direction of mean gradient in both NWM solutions was in a very good agreement with all GNSS post-processing variants.

Directions of mean gradient over individual stations were mostly within ±15° when compared to the total mean gradient estimated for the stations and the solution variant. On the other hand, the performance was not identical for the individual solutions. A change of cut-off elevation angle from 7° to 3° led to an increased number of stations with the mean gradient direction within ±15° of the total mean direction and to a decreased number of stations with a mean gradient direction differing for more than 30° (regarded as outlier stations in Table 2). Two GNSS stations were marked as outliers by all processed variants with their mean gradient direction differing by more than 50° from the total variant mean. Both of them are located in an urban area in south-west Germany and are using the same receiver and antenna type from Leica, which is however used by many other stations in the same region where no issues with gradient mean angle were identified. Still, the reason of their different behaving can be of instrumental or environmental origin.

Table 2. Mean magnitudes and azimuth angles of tropospheric gradients from all individual GNSS variants of processing and NWMs ERA5 and WRF.

Solution	Mean magnitude (mm)	Mean azimuth (°)	Percentage of stations with mean azimuth = total_mean ± 15°	Percentage of stations with mean azimuth = total_mean ± 30°	Number of outlier stations
GRCH3	0.82	170.0	89.7	99.2	2
GRBS3	0.67	170.2	92.6	98.8	3
GxCH3	0.83	168.2	88.5	97.5	6

GxCH7	0.86	168.0	73.7	95.5	11
GRCH7	0.84	170.2	79.0	97.1	7
RT1GxCH3	0.95	151.9	92.6	98.7	5
RT3GxCH3	1.18	162.7	96.3	98.8	3
RTEGxCH3	0.75	168.3	85.6	97.5	6
ERA5	0.68	169.3	96.3	100.0	0
WRF	0.73	170.9	100.0	100.0	0

Table 3 summarizes mean repeatability of daily coordinates as well as statistical comparison of formal errors of estimated ZTDs and tropospheric gradients from different GNSS processing variants. The station coordinates repeatability is improved when using combined GPS+GLONASS solutions compared to GPS-only solutions, namely by a factor of 2 and 1.2 in horizontal components and the height, respectively. The number of available satellites and their geometry plays a significant role in this context. An increase of the elevation angle cut-off (from 3° to 7°) resulted in improved height repeatability, which is consistent with the results of Zhou et al. (2017) suggesting optimal 7° cut-off for the height repeatability when comparing results of different elevation angle cut-off (3° - 15°). However, it should be noted that GPT+GMF models and the PPP method were used in both cases. Contrary, Douša et al. (2017) observed an improvement in the height repeatability even when using the elevation angle cut-off 3° (compared to 7° and 10°) when exploiting double-difference observations, the VMF1 mapping function (Boehm et al., 2006b) and the Bernese GNSS Software (Dach et al. 2015). Douša et al. (2017) indicated also worse results when using GPT+GMF compared to VMF1, which can be attributed to modelling errors in the former, particularly if applied in PPP (Kouba, 2009). We also notice a slightly better performance in case of the BS *mfq* when compared to the CH *mfq* while this difference was found to be statistically significant in the North and Up component by the Wilcoxon signed-rank test at the 5% significance level. The results of the forward filter processing didn't show any degradation when using the ESA final products (RTEGxCH3). When using the IGS real-time product, the repeatability of all coordinates got worse by a factor of 2-3 and 4-5 for RT1GxCH3 and RT3GxCH3 variant respectively. The latter is attributed to a lower quality of the IGS03 RT product during some periods, see Figure 4.

Formal error of the parameter can be generally regarded as an estimation uncertainty. Formal errors increase when the number of observations and/or the geometry decrease. Naturally, smaller formal errors correspond to the lower elevation angle cut-off, which can be observed for both ZTDs and tropospheric gradients in Table 3. Formal errors are about 17% and 11% smaller when using the 3° cut-off (GRCH3) compared to the 7° cut-off (GRCH7) for horizontal gradients and ZTDs, respectively, thus indicating a higher impact on the former. A decrease of formal errors of tropospheric gradients estimated with a 3° cut-off compared to 10° cut-off was previously reported also by Meindl et al. (2004). Interestingly, using the BS *mfq* resulted in smaller formal errors of tropospheric gradients, but we haven't observed any change in formal errors of other estimated parameters. The smaller formal errors may suggest an improvement in estimated parameters using BS *mfq*, as also found from the coordinates repeatability.

Table 3. Mean position repeatability and formal errors and their standard deviation for tropospheric parameters from individual GNSS processing variants.

GNSS solution	Position repeatability			ZTD formal error		N gradient formal error		E gradient formal error	
	North (mm)	East (mm)	Height (mm)	Mean (mm)	SD (mm)	Mean (mm)	SD (mm)	Mean (mm)	SD (mm)
GRCH3	1.71	4.13	5.60	3.80	0.37	0.81	0.10	0.81	0.09
GRBS3	1.69	4.13	5.53	3.82	0.37	0.74	0.09	0.75	0.09
GxCH3	3.62	8.68	5.91	4.28	0.46	0.93	0.13	0.90	0.13
GxCH7	3.46	9.26	5.43	4.84	0.44	1.14	0.14	1.05	0.14
GRCH7	1.71	4.09	4.96	4.28	0.36	0.99	0.10	0.95	0.11
RT1GxCH3	3.97	10.71	7.57	6.66	0.70	0.91	0.08	0.92	0.09
RT3GxCH3	9.13	19.69	8.51	7.05	0.80	1.49	0.22	1.53	0.22
RTEGxCH3	1.68	3.91	5.74	6.60	0.68	0.90	0.08	0.91	0.08

3.2~~1~~ Comparison of individual GNSS variants with each other

~~Absolute values of tropospheric gradient components stay typically below 1–2 mm under standard atmospheric conditions and can reach 4–6 mm during severe weather conditions. The gradient of 1 (6) mm corresponds to about 55 (330) mm slant delay correction when projected to 7° elevation angle. For an illustration an example time series of tropospheric gradients at station LDB2 (Brandenburg, Germany) for a period between May 15 and June 15, 2013 is given in Figure 2.~~

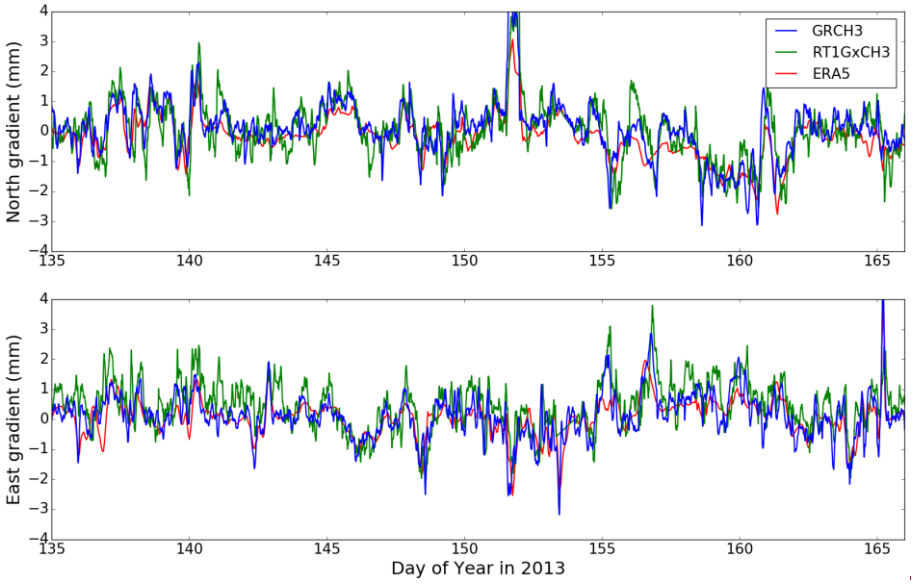

~~**Figure 2.** Tropospheric gradients retrieved from GNSS data processing (GRCH3, RT1GxCH3) and from NWM ERA5 at station LDB2 (52.209°N, 14.121°E, Germany) for a period from May 15, 2013 till June 15, 2013.~~

Results for individual GNSS variants comparison based directly on ~3.~~6~~ 4 million of pairs of values over 55 days and 243 GNSS stations are presented in Table 4~~2~~. We notice a good agreement among all the post-processing ~~(PP)~~ variants ~~from the statistics~~(top part of Table 4). The mean differences stayed below 0.2 mm for ZTD and ±0.02 mm for tropospheric gradients with one exception for the latter parameter. This was a comparison between results provided by CH and BS *mfg*s where the

mean differences reached -0.05 mm and 0.03 mm for north and east gradient component, respectively. These small systematic effects can be attributed to the average difference between tropospheric gradients computed with BS *mfg* compared to CH *mfg*.

The standard deviation (~~SDEV~~SD) indicates ~~a~~ the smallest ~~negligible~~ impact due to the change of *mfg* for both ZTD estimates (0.2 mm) and ~~the smallest impact on~~ tropospheric gradients (~0.14 mm). The impact increases then for both ZTD and gradients when comparing results of single and dual-constellation (1.2 mm for ZTD, ~0.~~18~~17 mm for gradients). It should be noted that GLONASS observations were down-weighted by a factor of 1.5 in dual-constellation variants of solution to reflect both a lower quality of precise products and observations. The gradients estimated with improved geometry and using more observations are expected to provide more accurate and reliable estimates. It is notable in the comparisons of single-/dual-constellation at different elevation cut-off angles (the impact is larger for a higher cut-off). The largest impact is eventually observed due to the elevation cut-off angle, i.e. 2.2 mm and ~0.~~21~~20 mm for ZTD and tropospheric gradients, respectively. Linear correlation coefficients (CorCoef) reach value of ~1 in all cases for the ZTD comparisons. The ZTDs were thus practically unaffected by different gradient models. For the gradient comparisons, the correlation coefficients are progressively decreasing from 0.99 to 0.95 while values of SD are increasing.~~By using common data, period, processing strategy and software in our analysis, a significance of the impact of different models can be assessed by confronting achieved SDEV with those obtained when comparing gradients from different software, processing methods and even observing techniques. Generally, the SDEV values in Table 2 reach 30-50% of those obtained from comparing two different GNSS software and processing methods with two different NWM sources, and still using the same data set from the benchmark campaign (Douša et al. 2016). Differences between ZTDs and tropospheric gradients from all compared variants of solution were also statistically tested. And in all cases, the differences were found to be statistically significant at the 5% significance level while using the Wilcoxon signed-rank test. This non-parametric test was used since none of the processed variant of solution evinced a normal distribution of their ZTDs and tropospheric gradients.~~

~~Linear correlation coefficients (CorCoef) reach value of 1.0 in all cases for the ZTD comparisons with an exception of 0.999 in case of standalone GPS solution and 7-deg elevation cut-off. The ZTDs were thus practically unaffected by different models. The correlation coefficients are then progressively decreasing from 0.99 to 0.95 for gradient comparisons when following trends described for results of SDEV. Generally, we observed very small mean differences in all the cases. Interestingly, comparing results with CH and BS *mfgs* provided the largest mean differences of -0.05 mm and 0.03 mm for north and east gradient component, respectively, although they fit the best in terms of SDEV and correlation coefficients compared to all other cases. These small systematic effects can be attributed to the average difference between tropospheric gradients computed with BS *mfg* compared to CH *mfg*. However, they are averaged over all stations and the period while they still strongly depend on both size and orientation of gradients as will be discussed in Section 4.~~

An increased scatter of RT processing is visible on significant mean differences and on the standard deviation values of ZTD and tropospheric gradients increased by a factor of 3 ~~and on significant mean differences~~. These are also emphasised by the reduction of correlation coefficients mainly for tropospheric gradients. The two RT solutions can be still considered of good quality if we take into consideration results found in Ahmed et al. (2016) or Kačmařík (2018), where mean biases and ~~SDEV~~

SD values up to 12 mm were reported for comparisons between RT ZTD solutions based on IGS01 and IGS03 streams and post-processing solutions based on final products. Since virtually zero mean differences for both ZTD and tropospheric gradients ~~were present~~are found in the RTEGxCH3 variant, when using the Kalman filter too, the degraded quality of RT tropospheric parameters is mainly a consequence of the poorer quality of IGS01 and IGS03 RT products (Douša et al., 2018b). The differences of ZTDs and tropospheric gradients from all compared variants of solution were also statistically tested. And in all cases, the differences were found to be statistically significant at the 5% significance level while using the Wilcoxon signed-rank test (https://docs.scipy.org/doc/scipy/reference/generated/scipy.stats.wilcoxon.html). This non-parametric test was used since none of the processed variant of solution evinced a normal distribution of their ZTDs and tropospheric gradients.

Table ~~4~~2. Comparison of individual variants of GNSS data processing run in post-processing mode (top) and in simulated real-time mode (bottom), units: Mean and ~~SDEV~~ SD in mm, CorCoef represents a linear correlation coefficient.

Compared ~~PP~~ post-processing solutions	ZTD			N-S gradient			E-W gradient		
	Mean	~~SDEV~~SD	CorCoef	Mean	~~SDEV~~SD	CorCoef	Mean	~~SDEV~~SD	CorCoef
GRCH3 – GRBS3	0.0	0.2	1.000	-0.05	0.~~15~~14	0.~~991~~995	0.03	0.13	0.~~995~~996
GRCH3 – GxCH3	0.1	1.1	1.000	0.00	0.~~17~~16	0.973~~0~~	-0.02	0.~~16~~15	0.~~973~~976
GRCH7 – GxCH7	0.1	1.2	1.000	-0.01	0.~~20~~19	0.~~961~~963	-0.02	0.~~18~~17	0.~~961~~968
GRCH3 – GRCH7	0.1	2.1	1.000	0.01	0.20	0.~~958~~961	0.00	0.18	0.~~964~~966
GxCH3 – GxCH7	0.2	2.2	~~0.999~~1.000	0.01	0.23	0.~~947~~949	-0.01	0.~~21~~20	0.~~954~~957

Compared RT solutions	ZTD			N-S gradient			E-W gradient		
	Mean	~~SDEV~~SD	CorCoef	Mean	~~SDEV~~SD	CorCoef	Mean	~~SDEV~~SD	CorCoef
RT1GxCH3-GxCH3	3.~~5~~4	5.~~9~~7	0.996	~~-~~0.10	0.~~55~~54	0.~~698~~716	~~-~~0.18	0.~~57~~55	0.~~648~~669
RT3GxCH3 - GxCH3	2.7	6.2~~4~~	0.996	~~-~~0.05	0.~~76~~66	0.699~~49~~	~~-~~ 0.~~08~~09	0.~~80~~68	0.~~584~~651
RTEGxCH3 - GxCH3	0.1	4.4	0.998	~~-~~0.00	0.39	0.8332~~7~~	~~-~~ 0.~~02~~01	0.~~44~~43	0.~~763~~776
RT1GxCH3 – RT3GxCH3	0.8	5.0	0.997	-0.0~~3~~5	0.~~75~~65	0.~~664~~718	0.~~11~~09	0.~~75~~63	0.712~~638~~

3.2 Comparison of individual GNSS variants with NWM

The statistics for the GNSS and NWM comparisons are summarized in Table ~~3~~5. For ZTDs ~~A~~ a mean difference of about 1 (4) mm is visible ~~for ZTDs~~ between GNSS and ERA5 with standard deviations around 9 (~~11~~10) mm and correlation coefficients around 0.99 (0.99) for individual ~~PP~~ post-processing (RT) GNSS solutions. The negative mean difference of -3 mm in ZTD between GNSS and WRF might be due to the global NCEP GFS analysis which is used for the initial and boundary conditions for the WRF solution. A negative mean difference of -5 mm in ZTD between two GNSS reference solutions and a solution based on the NCEP GFS was already reported in the past (Douša et al., 2016). The standard deviations of differences are about 2 mm larger when GNSS and WRF are compared. This is probably due to the fact that the solution from WRF is based on a 24-hour ~~free~~ forecast (errors are supposed to grow with increasing forecast length) whereas the solution from ERA5 is based

on a reanalysis. ~~The negative mean difference of -3 mm in ZTD between GNSS and WRF might be due to the global NCEP GFS analysis which is used for the initial and boundary conditions for the WRF solution. A negative mean difference of -5 mm in ZTD between two GNSS reference solutions and a solution based on the NCEP GFS was already reported in the past (Douša et al., 2016).~~

Table ~~3~~5. Comparison of individual variants of GNSS data processing run in post-processing mode (top) and in simulated real-time mode (bottom) with NWM solutions, units: Mean and ~~SDEV~~ SD in mm, CorCoef represents a linear correlation coefficient.

Compared ~~PP~~ post-processing solutions	ZTD			N-S gradient			E-W gradient		
	Mean	~~SDEV~~SD	CorCoef	Mean	~~SDEV~~SD	CorCoef	Mean	~~SDEV~~SD	CorCoef
GRCH3 – ERA5	1.0	8.8	0.992	-0.02	0.~~47~~46	0.743~~25~~	-0.01	0.~~47~~46	0.744~~21~~
GRBS3 – ERA5	1.0	8.9	0.992	0.~~04~~03	0.~~42~~41	0.730~~14~~	-0.03	0.~~43~~42	0.729~~08~~
GxCH3 – ERA5	~~0.9~~1.0	9.~~1~~0	0.991	-0.01	0.~~49~~47	0.727~~03~~	0.01	0.~~48~~46	0.737~~09~~
GxCH7 – ERA5	0.7	10.~~2~~0	0.989	-0.02	0.~~56~~54	0.653~~24~~	0.02	0.~~53~~51	0.685~~52~~
GRCH7 – ERA5	0.~~9~~8	9.~~8~~7	0.990	-0.~~03~~02	0.~~54~~51	0.680~~55~~	-0.00	0.~~51~~50	0.699~~72~~
GRCH3 – WRF	-~~3.0~~2.8	11.~~3~~1	0.987	-0.04	0.~~54~~51	0.688~~54~~	0.~~01~~00	0.~~56~~52	0.~~630~~681
GRBS3 – WRF	-2.~~9~~7	11.~~3~~2	0.98~~76~~	0.01	0.~~49~~47	0.675~~43~~	-0.02	0.~~52~~49	0.664~~18~~
GxCH3 – WRF	-~~3.0~~2.8	11.~~5~~3	0.98~~67~~	-0.04	0.~~56~~52	0.~~633~~673	0.02	0.~~57~~53	0.~~621~~675
GxCH7 – WRF	-3.~~2~~1	1~~2.3~~1.9	0.~~984~~985	-0.~~05~~04	0.~~62~~58	0.~~564~~611	0.03	0.~~61~~56	0.~~573~~632
GRCH7 – WRF	-~~3.1~~2.9	~~12~~11.~~07~~	0.985	-0.05	0.~~59~~56	0.~~592~~633	0.01	0.~~59~~55	0.~~589~~644

Compared RT solutions	ZTD			N-S gradient			E-W gradient		
	Mean	~~SDEV~~SD	CorCoef	Mean	~~SDEV~~SD	CorCoef	Mean	~~SDEV~~SD	CorCoef
RT1GxCH3 – ERA5	4.4	10.~~5~~1	0.98~~98~~	-0.12	0.~~59~~55	0.~~606~~650	0.~~19~~20	0.~~58~~56	0.~~578~~621
RT3GxCH3 – ERA5	3.~~6~~4	10.~~9~~3	0.~~988~~989	-~~0.07~~05	0.~~85~~71	0.~~504~~573	0.~~08~~11	0.~~87~~72	0.~~456~~573
RTEGxCH3 – ERA5	1.0	9.~~7~~6	0.990	-0.01	0.~~47~~46	0.~~692~~713	-~~0.01~~00	0.~~46~~45	0.~~680~~714
RT1GxCH3 – WRF	0.~~57~~5	12.~~6~~1	0.98~~43~~	-0.14	0.~~65~~59	0.~~544~~610	0.~~21~~20	0.~~65~~61	0.~~504~~560
RT3GxCH3 – WRF	-0.~~3~~4	12.~~9~~2	0.98~~42~~	-~~0.09~~07	0.~~89~~74	0.~~537451~~	0.~~10~~12	0.~~92~~76	0.~~523391~~
RTEGxCH3 – WRF	-2.~~9~~7	~~12~~11.~~06~~	0.98~~65~~	-0.04	0.~~54~~50	0.66~~827~~	0.01	0.~~54~~51	0.~~647597~~
ERA5 ~~–~~ – WRF	-3.9	11.1	0.987	-0.02	0.40	0.771	0.01	0.44	0.722

With regards to the tropospheric gradients, the mean differences between post-processed GNSS and NWM stayed within a range from -0.05 to 0.0~~3~~4 mm ~~(with the exception of the GNSS RT solutions)~~. ~~Here the~~ The existing differences between two GNSS variants of solution based on different *mfg*s can be attributed to usage of CH *mfg* for derivation of NWM tropospheric gradients and to the existing systematic difference between tropospheric gradients estimated using these two *mfg*s (see Section 2.2 and Appendix A). The standard deviations between GNSS and NWM were approximately doubled or tripled when compared to standard deviations between individual variants of GNSS solutions (Table 4). They were also found to be higher

for the WRF than for ERA5. Again, this can be probably explained by the fact that the solution from WRF is based on a 24-hour free forecast whereas ERA5 is based on a reanalysis.

~~In order to evaluate the statistical significance of differences between ZTDs and tropospheric gradients from all variants of GNSS solution and both NWMs we realized the same statistical tests as mentioned in the previous section. Again, the differences were found to be statistically significant at the 5% significance level in all cases.~~

~~NWMs obviously cannot be regarded as representing ground truth atmospheric conditions. However, a similar pattern is present in results for both of them~~Both NWMs lead to consistent results: standard deviations are smaller and correlation coefficients higher for GNSS solutions using a lower cut-off elevation angle (3° instead of 7°) and/or ~~when using~~ more observations (GPS+GLONASS). For example, the ~~SDEV~~ SD for north gradient component between GNSS and ERA5 is 0.5~~6~~4 mm for the GxCH7 variant while 0.4~~6~~7 mm for the GRCH3 variant. This represents a decrease of 1~~6~~5 %. In this regards we also derived tropospheric parameters from both NWMs using a 7° cut-off elevation angle and repeated the comparisons to test if GNSS variants of solution with a 7° cut-off would be closer to NWM solutions based also on the 7° cut-off angle. And we always found a better agreement between any evaluated GNSS variant of solution and the NWM solution based on the 3° cut-off angle – in terms of mean difference, standard deviation and correlation coefficient. ~~It indicates that the settings of cut-off elevation angle in NWM ray-tracing does not influence the described pattern in GNSS results.~~ From two GNSS variants differing only in the *mfg*, the solution applying the BS mapping function is closer to the NWMs in terms of standard deviation. Since the CH *mfg* was used to derive tropospheric gradients from NWMs, the opposite situation could be expected, and we generally note that presented results of comparisons between tropospheric gradients from the GNSS GRBS3 solution and NWMs should be taken only as informative. The lower values of standard deviation can be partly understood as the magnitudes computed as $\sqrt{Gn^2 + Ge^2}$ of GNSS tropospheric gradients using the BS *mfg* are smaller compared to the CH *mfg* (see Section 2.2) and the magnitudes of NWM tropospheric gradients are more smoothed compared to the GNSS tropospheric gradients.

In order to evaluate the statistical significance of differences of ZTDs and tropospheric gradients from all variants of GNSS solution and both NWMs we applied again the Wilcoxon signed-rank test. Again, the differences were found to be statistically significant at the 5% significance level in all cases.

Maps showing tropospheric gradients were generated for all the variants of GNSS solutions and both NWM solutions and visually evaluated for the whole benchmark period. For better visualization we included all the GNSS stations of the benchmark campaign, i.e. not just the subset of 243 stations used for the presented statistics. Generally, GNSS provided homogenous fields of tropospheric gradients without a noisy behaviour at the level of individual stations and a very good agreement in gradient directions and usually also in gradient magnitudes was found between GNSS and NWM gradient maps. In Figure 3, two examples are shown for different events when weather fronts were passing over the studied area. For a description of meteorological conditions prevailing during these events the reader is referred to Douša et al. (2016). Tropospheric gradients derived from NWM provided more smoothed gradient fields, but somehow limited to render local structures mainly due to the spatial resolution of both NWMs. As the ERA5 model has coarser spatial resolution than the WRF model, such behaviour was

a little bit more apparent in its ~~outputs~~results. On the other hand, when compared to results of the 1° × 1° resolution global models ERA-Interim and NCEP GFS (Douša et al., 2016), the presented NWMs tropospheric gradients have larger magnitudes.

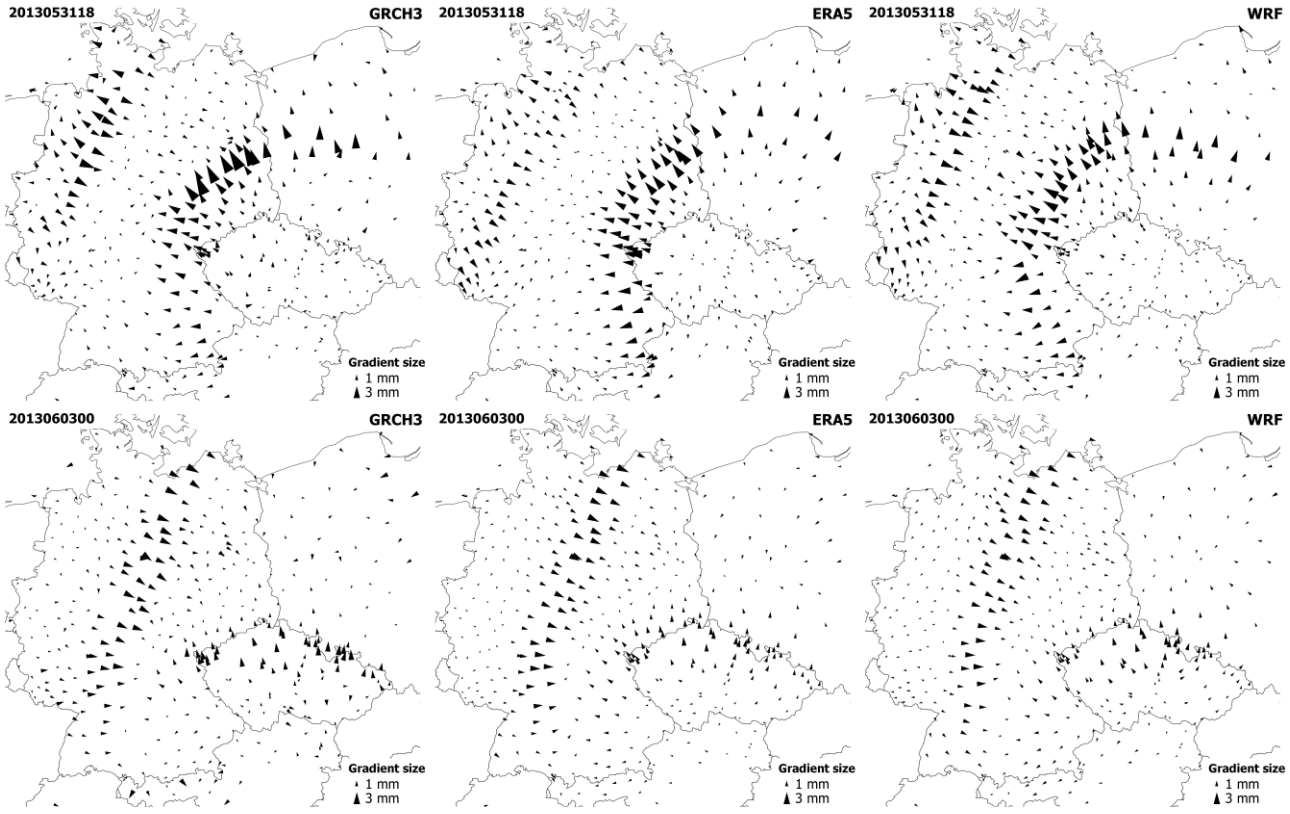

Figure 3. Tropospheric gradient maps from GNSS GRCH3 solution (left), NWM ERA5 solution (middle) and NWM WRF solution (right) on 31 May 2013, 18:00 UTC (top) and on 03 June 2013 00:00, UTC (bottom).

Comparing GNSS to NWM products in Table 5~~3~~ indicated that the RTEGxCH3 solution driven by the Kalman filter and the ESA final product shows a comparable performance to the GxCH3 solution driven by the Kalman filter and the backward smoother. An increase of mean difference and standard deviation values for other solutions based on RT mode indicates that the quality of the RT tropospheric solution is dominated by an actual quality of RT orbit and clock corrections. In this regard, we examined systematically all tropospheric gradient maps and found that gradients from the RTEGxCH3 solution are always in a very good agreement with ~~PP~~ post-processing solutions. Although there were imperfections in matching RT1GxCH3 gradients and post-processing ~~PP~~ solutions, the performance can be still considered as generally good and stable. This was however not the case of the RT3GxCH3 solution where we observed a varying quality of estimated tropospheric gradients. For the majority of epochs, in particular during the periods with strong gradients, the tropospheric gradients could be evaluated as acceptable. However, situations when gradients from all the stations point to the same direction occurred from time to time, obviously without a physical relation to the actual weather situation. An example of this behaviour is presented in Figure 4 where tropospheric gradients from the RT3GxCH3 solution behave normally on 31 May 2013, 18:00 UTC, and became

unrealistic on 6 May 2013, 18:00 UTC where all the stations point to the south-west direction and reveal high gradient magnitudes. Such issues occurred occasionally for a limited period of time in the RT3GxCH3 solution only. The reason is an instability of the RT3 stream during the initial period (the first half of 2013) affected by many interruptions and data gaps thus caused frequent parameter re-initialization in PPP.

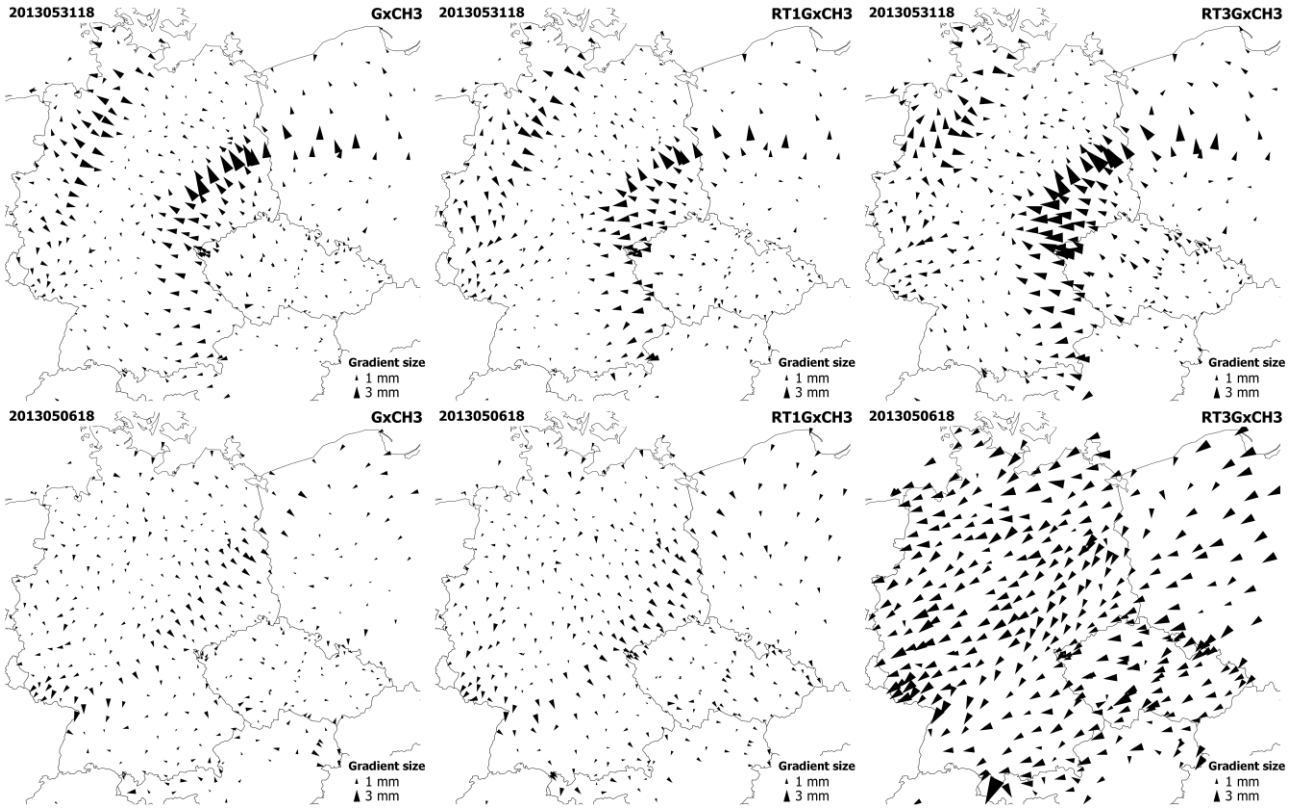

Figure 4. Tropospheric gradient maps from GNSS GxCH3 solution (left), GNSS RT1GxCH3 solution (middle) and GNSS RT3GxCH3 solution (right) on 31 May 2013, 18:00 UTC (top) and on 06 May 2013, 18:00 UTC (bottom).

~~**3.3 Additional assessment of processing settings on GNSS tropospheric gradients**~~

~~Mean gradient magnitudes and azimuth angles (direction of gradient) over the whole benchmark period were computed for 243 GNSS stations and are presented in Table 4. Mean magnitudes of tropospheric gradients from all PP GNSS variants oscillated around 0.85 mm and 0.67 mm when using the CH *mfg* and the BS *mfg*, respectively. Gradients computed using the latter show about 17 % smaller gradients compared to the former if all the processing aspects remained identical. Both RT solutions also resulted with higher gradient magnitudes, namely +14 % for RT1GxCH3 and +47 % for RT3GxCH3 when compared to the corresponding GxCH3 PP variant. A mean gradient magnitude of about 0.7 mm was found for both NWM solutions, i.e. of about 0.1 mm smaller than for the GRCH3 solution. This can be mainly explained by the limited horizontal resolution of the NWMs.~~

Table 4 shows that mean tropospheric gradients point towards the equator what is in an agreement with Meindl et al. (2004). Such a mean gradient direction does not depend on the gradient mapping function. By adding GLONASS observations the mean gradient direction was changed by +2°, however, actual effects were found to be highly station dependent with a typical range of ±5° for individual stations. The direction of mean gradient in both NWM solutions was in a very good agreement with all GNSS post-processing variants.

Directions of mean gradient over individual stations were mostly within ±15° when compared to the total mean gradient estimated for the stations and the solution variant. On the other hand, the performance was not identical for the individual solutions. A change of cut-off elevation angle from 7° to 3° led to an increased number of stations with the mean gradient direction within ±15° of the total mean direction and to a decreased number of stations with a mean gradient direction differing for more than 30° (regarded as outlier stations in Table 4). Two GNSS stations were marked as outliers by all processed variants with their mean gradient direction differing by more than 50° from the total variant mean. Both of them are located in an urban area in south-west Germany and are using the same receiver and antenna type from Leica, which is however used by many other stations in the same region where no issues with gradient mean angle were identified. Still, the reason of their different behaving can be of instrumental or environmental origin.

Table 4. Mean magnitudes and azimuth angles of tropospheric gradients from all individual GNSS variants of processing and NWMs ERA5 and WRF.

Solution	Mean magnitude (mm)	Mean azimuth (°)	Percentage of stations with mean azimuth = total_mean ± 15°	Percentage of stations with mean azimuth = total_mean ± 30°	Number of outlier stations
GRCH3	0.81	170.3	88.9	99.2	2
GRBS3	0.67	170.4	91.8	98.8	3
GxCH3	0.83	168.4	88.1	97.5	6
GxCH7	0.86	168.2	74.1	95.1	12
GRCH7	0.84	170.5	79.8	97.1	7
RT1GxCH3	0.95	152.4	92.6	97.9	5
RT3GxCH3	1.22	162.7	96.3	98.8	3
RTEGxCH3	0.75	168.7	86.0	97.5	6
ERA5	0.68	169.4	96.3	100.0	0
WRF	0.73	171.0	100.0	100.0	0

Table 5 summarizes mean repeatability of daily coordinates as well as statistical comparison of formal errors of estimated ZTDs and tropospheric gradients from different GNSS processing variants. The station coordinates repeatability is improved when using combined GPS+GLONASS solutions compared to GPS only solutions, namely by a factor of 2 and 1.2 in horizontal components and the height, respectively. The number of available satellites and their geometry plays a significant role in this context. An increase of the elevation angle cut-off (from 3° to 7°) resulted in improved height repeatability, which corresponds to Zhou et al. (2017) suggesting optimal 7° cut-off for the height repeatability when comparing results of different

elevation angle cut-off (3° - 15°). However, it should be noted that GPT+GMF models and the PPP method were used in both cases. Contrary, Douša et al. (2017) observed an improvement in the height repeatability even when using the elevation angle cut-off 3° (compared to 7° and 10°) when exploiting double-difference observations, the VMF1 mapping function (Boehm et al., 2006b) and the Bernese GNSS Software (Dach et al. 2015). This discrepancy might be attributed to a slightly worse modelling of low elevation observations when using the GPT+GMF, in particular when the PPP strongly depends on all modelling aspects of undifferenced observations. We also notice a slightly better performance in case of the BS *mfg* when compared to the CH *mfg*. The results of the forward filter processing didn't show any degradation when using the ESA final products (RTEGxCH3). When using the IGS real-time product, the repeatability of all coordinates got worse by a factor of 2-3 and 4-5 for RT1GxCH3 and RT3GxCH3 variant respectively. The latter is attributed to a lower quality of the IGS03 RT product during some periods, see Figure 4.

Formal error of the parameter can be generally regarded as an estimation uncertainty. Typically, high formal errors for tropospheric parameters occur at situations when estimated under unfavourable conditions, e.g. low number of observations and/or their poor geometry and/or their poor quality. Naturally, smaller formal errors correspond to the lower elevation angle cut-off, which can be observed for both ZTDs and tropospheric gradients in Table 5. Formal errors are about 17% and 11% smaller when using the 3° cut-off (GRCH3) compared to the 7° cut-off (GRCH7) for horizontal gradients and ZTDs, respectively, thus indicating a higher impact on the former. A decrease of formal errors of tropospheric gradients estimated with a 3° cut-off compared to 10° cut-off was previously reported also by Meindl et al. (2004). Interestingly, using the BS *mfg* resulted in smaller formal errors of tropospheric gradients, but we haven't observed any change in formal errors of other estimated parameters. The smaller errors may suggest an improvement in estimated parameters, i.e. see coordinates repeatability, but it can be also partly attributed to the different *mfg* coefficients.

Table 5. Mean position repeatability and formal errors and their standard deviation for tropospheric parameters from individual GNSS processing variants.

GNSS solution	Position repeatability			ZTD formal error		N gradient formal error		E gradient formal error	
	North (mm)	East (mm)	Height (mm)	Mean (mm)	SDEV (mm)	Mean (mm)	SDEV (mm)	Mean (mm)	SDEV (mm)
GRCH3	1.71	4.13	5.60	3.81	0.37	0.81	0.10	0.81	0.09
GRBS3	1.69	4.13	5.53	3.82	0.37	0.74	0.09	0.75	0.09
GxCH3	3.62	8.68	5.91	4.28	0.46	0.93	0.13	0.90	0.13
GxCH7	3.46	9.26	5.43	4.84	0.44	1.14	0.14	1.05	0.14
GRCH7	1.71	4.09	4.96	4.28	0.36	0.99	0.10	0.95	0.11
RT1GxCH3	3.97	10.71	7.57	6.71	1.72	0.91	0.08	0.92	0.09
RT3GxCH3	9.13	19.69	8.51	7.09	1.76	1.50	0.22	1.53	0.22
RTEGxCH3	1.68	3.91	5.74	6.60	0.67	0.91	0.08	0.92	0.08

4 Systematic effects induced by different gradient mapping functions and elevation-dependent weighting~~of GNSS tropospheric gradients estimation~~

In this section, we focus on studying systematic differences induced purely by ~~utilizing~~ different *mfg* and observation elevation-dependent weighting (OEW) during eight days from May 25 to June 1, 2013. For two solutions defined in Section 2.2 and utilizing CH *mfg* (GRCH3) and BS *mfg* (GRBS3), we additionally generated four variants using various OEW schemes: 1) EQUAL, equal weighting, 2) SINEL1, $1/sin(e)$, 3) SINEL2, $1/sin^2(e)$, and 4) SINEL4, $1/sin^4(e)$. Generally, in the SINEL OEW schemes, ~~T~~the contribution of low-elevation observations to all estimated parameters decreases with increasing power y in $1/sin^y(e)$.

~~As a consequence, the magnitude of tropospheric gradients is reduced due to the strong dependence on such observations. The impact of the *mfg* on the estimated tropospheric gradients is then reduced too.~~ Figure 5 displays example distributions of carrier-phase post-fit residuals with respect to the elevation for the SINEL2 observation weighting (left panel), and without any weighting, i.e. EQUAL (right panel). While the residuals from the former are affected by the *mfg* only below 15° elevation, the residuals in the latter are affected at any elevation angles even close to the zenith direction. Above the 30° elevation, the residuals distribution is more smoothed for the SINEL2 compared to the EQUAL. It is closer to the expected behaviour when considered errors in GNSS observations and models, including contributions from the atmosphere, multipath, uncertainty of receiver antenna phase centre variations, lower signal-to-noise ratio or cycle slips. All these errors generally increase with a decrease of observation elevation angle and, accordingly, minimum errors are thus expected in the zenith direction. The plots are also in agreement with our previous findings when studying extensively the distribution of carrier-phase post-fit residuals (not shown here for brevity sake). Using a weak or none elevation dependent weighting, the hydrostatic/wet delay mapping separation errors can introduce significant errors in both ZTD and height coordinate component (Kouba, 2009). Thought we generally recommend the use of SINEL2 elevation weighting, we show below also impact of other weighting schemes on estimated gradients. ~~These variants were provided for May 31, 2013 which is an interesting day due to an occlusion front present over Germany and captured by strong tropospheric gradients both from GNSS and NWM.~~

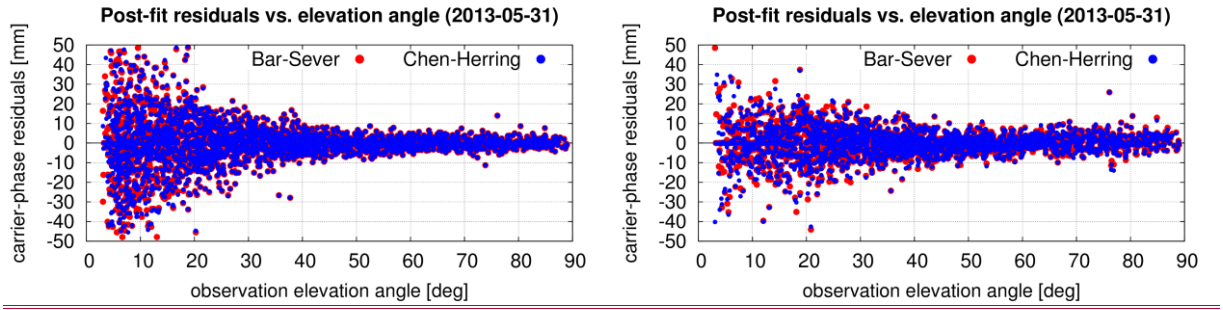

Figure ~~7~~5. Post-fit phase residuals distribution when using different gradient mapping functions, Bar-Sever (red) and Chen and Herring (blue), and observation weighting: SINEL2 (left) and EQUAL (right).

Figure 6 displays maps of situation with large tropospheric gradients observed on May 31, 2013 at 18:00 UTC when using GRCH3 (left panels) and GRBS3 (right panels) solutions and applying the SINEL2 OEW scheme. The day is interesting due

to a presence of occlusion front over Germany clearly captured by strong tropospheric gradients achievable from both GNSS and NWM analyses. The impact of *mfg* on estimated gradients shows systematic changes in gradient magnitudes – the gradients estimated with CH *mfg* (left panels) are always larger than with BS *mfg* (right panels) independently of the OEW scheme (not showed). It should be also noticed here, that the magnitudes of gradients estimated using the SINEL4 scheme were significantly reduced compared to any other OEW scheme.

Figure 7 shows mean differences, calculated over all epochs in May 31, 2013, in north (left panels) and east (right panels) gradient components between the two *mfg* (BS minus CH) when using the SINEL2 scheme. Although the magnitudes of CH gradients are always larger compared to BS gradients, the sign of the component differences depends on the gradient direction (north/south for *Gn* and east/west for *Ge*). Positive differences in north and east component appear when the estimated gradients point to south and west, respectively, and negative differences occur when the gradients point to opposite directions.

~~Figure 5 displays maps of tropospheric gradients on May 31, 2013 (18:00 UTC) from both GRCH3 (left panels) and GRBS3 (right panels) solutions when applying EQUAL, SINEL, SINEL2 and SINEL4 OEW schemes (panel rows from top to bottom). We can observe that OEW impacts magnitudes of gradients, but not much their directions. Magnitudes of individually estimated gradients from nearby stations show better consistency when using any real weighting compared to the EQUAL weighting suggesting a better quality of such product. This is also in agreement with our previous findings when studying the distribution of post-fit carrier-phase residuals with respect to the elevation angle (not showed). We achieved better performance when using SINEL2 scheme and worse when using EQUAL elevation-dependent weighting, see below in this section. The impact of *mfg* on estimated gradients clearly shows then systematic differences in magnitudes of gradients when considering different OEW schemes, compare panels from top to bottom. The gradients estimated with CH *mfg* (left panels) are then always larger than with BS *mfg* (right panels), independently of OEW used. We can also notice the gradient maps from SINEL and SINEL2 are very similar. The SINEL4 weighting then shows highly reduced gradient values indicating a strong impact of the low-elevation observations on their estimates.~~

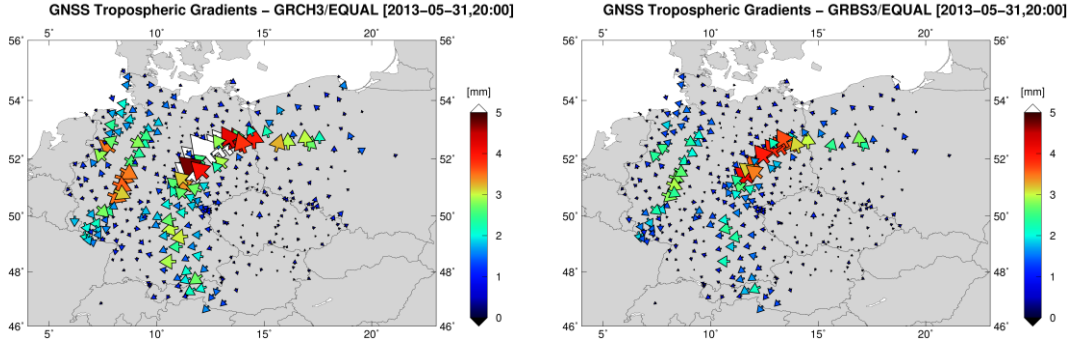

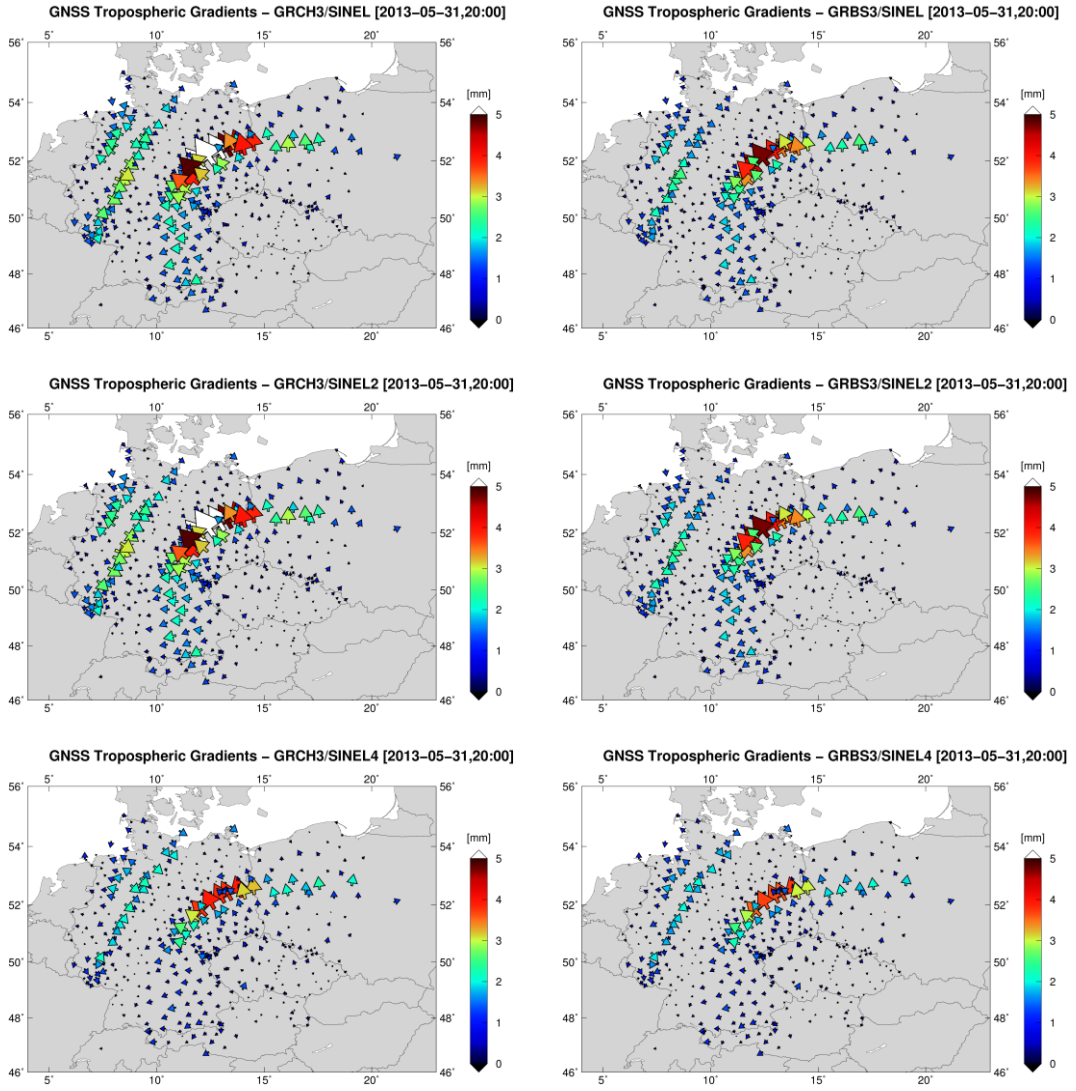

Figure ~~5~~6. Tropospheric gradient maps on May 31, 2013 (18:00 UTC) from GNSS solutions using the SINEL2 observation weighting scheme: Chen and Herring *mfg* (left panels), Bar-Sever *mfg* (right panels) ~~and EQUAL, SINEL, SINEL and SINEL4 (from top to bottom panels) observation weighting schemes~~.

~~Figure 6 shows mean differences (over all epochs in May 31, 2013) in north (left panels) and east (right panels) gradient components between the two *mfg* (BS *mfg* minus CH *mfg*) when using all OEW schemes. Such differences depend on both the magnitude and direction of estimated gradients when these are decomposed into two components. In our case, positive differences in north and east component appear when the estimated gradients point to south and west, respectively, and negative differences occur when the gradients point to opposite directions. Largest differences were observed for EQUAL weighting (top panels), which gradually decreased for SINEL, SINEL2 (next panel rows) and almost disappeared for SINEL4 (bottom panels).~~

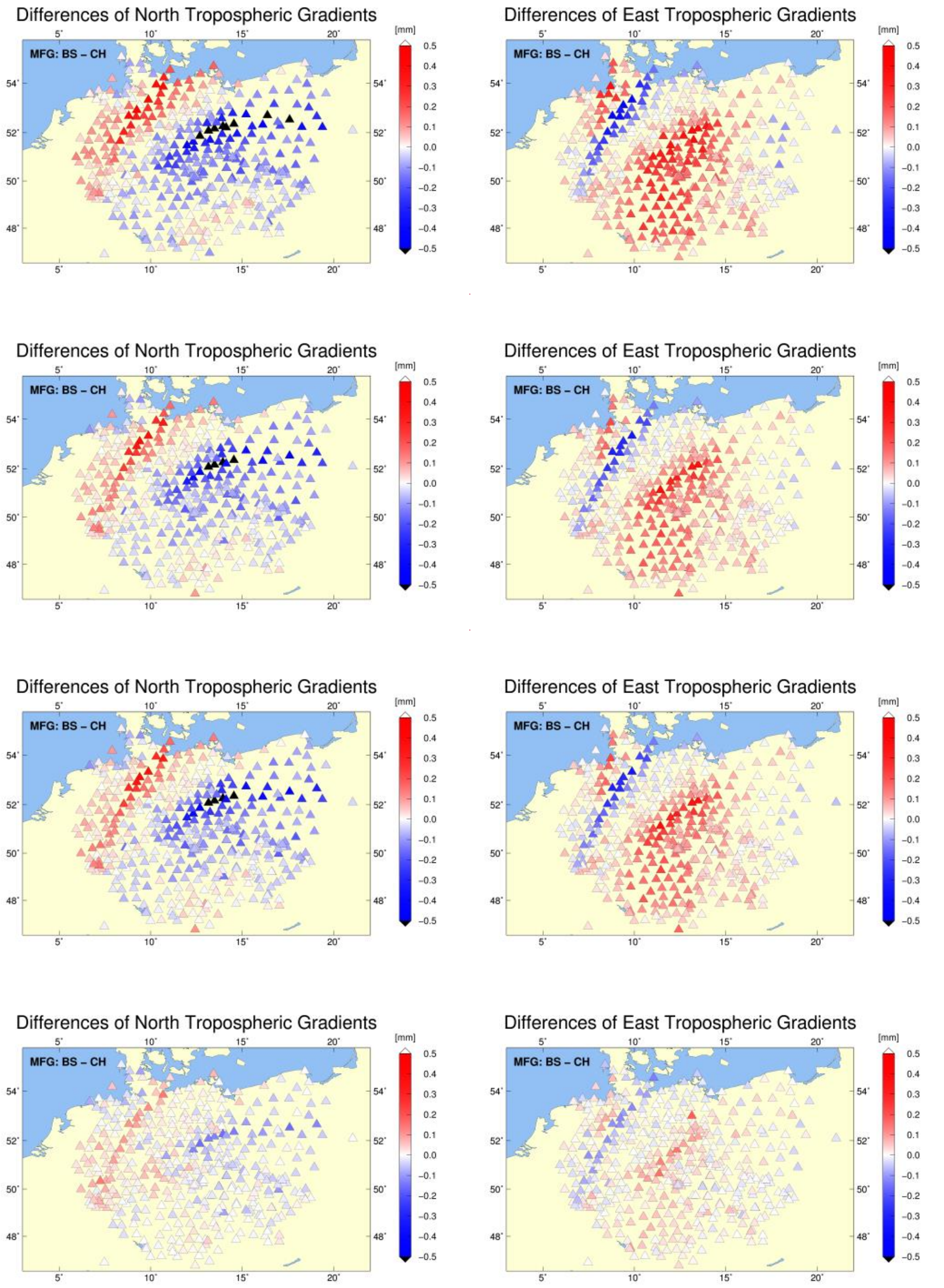
Differences of North Tropospheric Gradients
Differences of East Tropospheric Gradients
MFG: BS – CH
[mm]
0.5
0.4
0.3
0.2
0.1
0.0
−0.1
−0.2
−0.3
−0.4
−0.5
5°
10°
15°
20°
48°
50°
52°
54°

Figure ~~6~~7. Mean differences (calculated over full day May 31, 2013) of tropospheric gradient north component (left panels) and east component (right panels) due to different *mfg*: Chen and Herring (CH), Bar-Sever (BS) when using the ~~EQUAL, SINEL,~~ SINEL2 ~~and SINEL4 (from top to bottom panels)~~ observation weighting schemes. ~~Mean differences are calculated over full day May 31, 2013.~~

Figure 8 shows scatter plots of tropospheric gradient differences of all the stations in the network when using different *mfg* and OEW schemes on May 31, 2013. Obviously, the impact of the *mfg* on estimated gradients is significantly reduced for SINEL4 (well below 0.2 mm), while it is higher for all other schemes. This corresponds to the fact that large gradients are related to a horizontal anisotropy of the troposphere affecting more significantly low-elevation observations. The strongest effect can be observed for the EQUAL scheme reaching systematic differences of 1.0 mm or even higher. Such systematic differences reached twofold values of the SD obtained from comparisons of gradients using independent sources such as GNSS and NWM, see Section 3.3 or Douša et al. (2017).

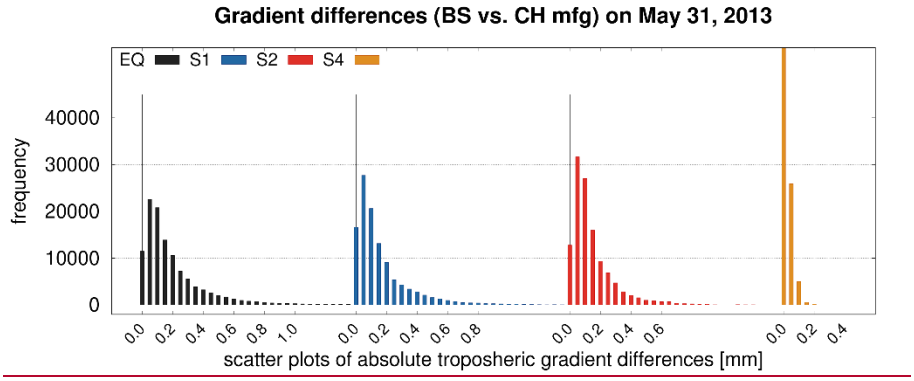

Figure 8. Differences of tropospheric gradients between Chen and Herring and Bar-Sever *mfg* for four observation weighting schemes: EQUAL (EQ), SINEL (S1), SINEL2 (S2), and SINEL4 (S4).

Figure 9 compares magnitudes of estimated gradients (east component only) and corresponding scatter plots of total gradient differences over all stations in the network on eight consecutive days (May 25 – June 1, 2013) when using CH and BS *mfg* and the SINEL2 OEW scheme. We can notice the days with a stronger tropospheric anisotropy (May 27-28, May 31, June 1) identifiable by a presence of gradients larger than 1.0 mm. The scatter plots systematically deviate from the zero on some days, prevailing negative and positive east components indicate that gradients in the network point westwards and eastwards, respectively. Differences in gradient magnitudes are then showed in the bottom panel. The impact due to utilizing different *mfg* clearly corresponds to the original gradient magnitudes. Both are high during the days with a strong tropospheric anisotropy, while differences due to the *mfg* choice demonstrate systematic effects up to 1 mm or more in such extreme cases.

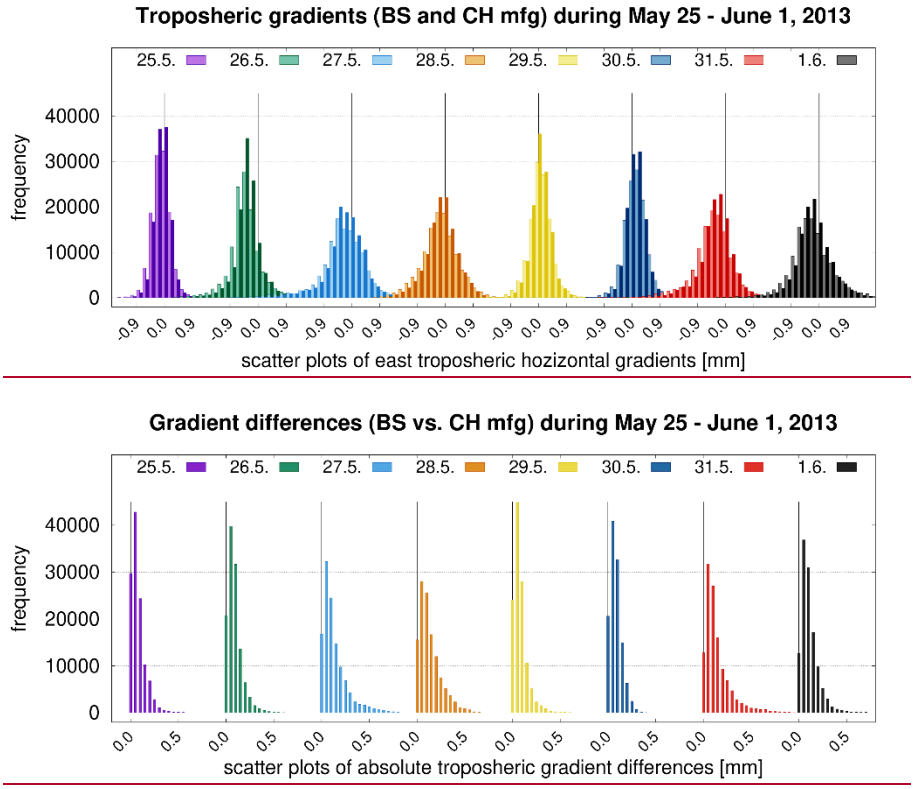

Figure 9. East tropospheric horizontal gradients (top) estimated using Chen and Herring (light columns) and Bar-Sever (dark columns) *mfg* and the differences (bottom) of gradients magnitudes between them. The SINEL2 OEW scheme was applied over eight days in May/June 2013.

~~Figure 7 finally displays carrier-phase post-fit residuals with respect to the elevation for selected solutions. The SINEL2 OEW scheme in the left panel shows more homogenous distribution of carrier-phase post-fit residuals above the elevation angle of 30° when compared to the EQUAL scheme (right panel). While the *mfg* selection impacts SINEL2 residuals on a few millimetre level below 15°, the EQUAL residuals could be affected at any elevation angles even up to the zenith direction. The SINEL2 resulted in a distribution of the post-fit residual reflecting the expectation due to contributing errors in both GNSS observations and models. The errors generally increase with a decrease of the elevation angle, and the lowest contribution is expected at the zenith. The effects of errors include contributions from the atmosphere, multipath, uncertainty of receiver antenna phase centre variations, lower signal-to-noise ratio or cycle slips.~~

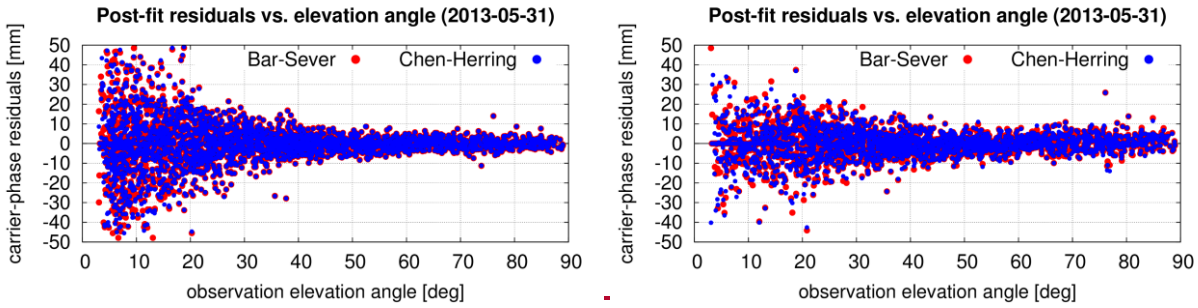

~~**Figure 7.** Post-fit phase residuals distribution when using different gradient mapping functions, Bar-Sever (red) and Chen and Herring (blue), and observation weighting: SINEL2 (left) and EQUAL (right).~~

5. Conclusions

We presented an impact assessment of selected GNSS processing settings on estimated tropospheric gradients together with an evaluation of ~~systematic~~ differences resulting from gradient mapping function and observation elevation weighting. We exploited the GNSS4SWEC benchmark campaign covering May and June in 2013 with prevailing wet weather ~~when the GNSS tropospheric gradients could provide a valuable information for meteorological applications~~. Although the time period covered some severe weather events, it also contained a lot of days with standard weather conditions with tropospheric gradients close to zero. Presented results could be therefore considered representative for European conditions during the warmer part of the year.

ZTD values and tropospheric gradients were estimated in eight variants of GNSS data processing and derived from two NWMs (a global reanalysis and a limited area short range forecast). All solutions gave tropospheric parameters in high temporal resolution (5 minutes). Since no meteorological data providing any information about prevailing atmospheric conditions during the evaluated time period entered the GNSS data processing, estimated tropospheric gradients can be regarded as fully independent, and therefore can provide additional interesting information, along with the ZTD, in support of NWMs (see Douša et al., 2016, Guerova et al., 2016).

~~A positive impact of a~~When lower~~ing~~ elevation angle cut-off (from 7° to 3°), more accurate ~~suggested more robust~~ tropospheric gradient estimates were obtained. ~~A 10% reduction in~~The standard deviation of differences of ~~was obtained when comparing~~ GNSS gradients to NWM gradients were reduced by 10%, ~~, and also by analysing~~ formal errors of tropospheric gradients were reduced and station-wise mean gradient directions were also more stable. On the other hand, the usage of lower cut-off angle led to a slightly worse station height repeatability (10 %), which is partly in contradiction ~~to~~ with the results of ~~achievements from~~ Douša et al. (2017~~). ~~)~~, but in agreement ~~However, our results agree~~ with Zhou et al. (2017). ~~and t~~The discrepancy is attributed to the use of PPP method with simplified modelling (GPT+GMF) for low-elevation observations. The 3° elevation angle cut-off can be ~~thus~~ nevertheless recommended for an optimal gradient estimation from GNSS data.

A small decrease of standard deviation of estimated gradients (2 %) was ~~achieved~~ observed when using GPS+GLONASS instead of GPS only and compared to NWM gradients. This indicates that the post-processing tropospheric gradients can be

reliably estimated solely with GPS constellation. However, it may still depend on applied software, strategy, products and processing, e.g. (near) real-time. In this regard, Li et al. (2015) and Lu et al. (2016) demonstrated that tropospheric gradients from multi-GNSS PPP processing improved their agreement with those estimated from NWM and WVR when compared to standalone GPS processing.

Using a simulated real-time processing mode, the agreement of GNSS versus NWM tropospheric gradients revealed an increase in standard deviation of about ~~17~~ 19 % (~~75~~ 53 %) for IGS01 (IGS03) RT products when compared to the corresponding GNSS post-processing gradients. We also show that the quality of real-time tropospheric parameters is dominated by the quality of real-time orbit and clock corrections, and to a much lesser extent by the processing mode, i.e. Kalman filter without backward smoothing. Tropospheric gradients from the RT solution using the IGS03 RT product showed occasionally a large misbehaving of tropospheric gradients at all GNSS stations obviously not related to weather conditions. This was caused by frequent PPP re-initializations due to interruptions and worse quality of the IGS03 RT product, while normal results were achieved by using the IGS01 RT product. Thus, providing high-resolution gradients in (near) real-time solution still remains challenging, which would require optimally a multi-GNSS constellation and high-accuracy RT products.

We studied systematic differences in estimated tropospheric gradients. Unlike for ZTDs, average systematic differences up to 0.5 mm over ~~one~~ a day, and up to ~~0.9~~1.0 mm or even more for individual gradient components during extreme cases, can affect the magnitude of estimated tropospheric gradients solely due to utilizing different gradient mapping functions or observation elevation-dependent weightings. ~~This difference was observed between Bar-Sever and Chen and Herring *mfg* while the tilting *mfg* behaves in between these two.~~ While the *mfg* choice affects the magnitude of estimated gradient, it does not affect the direction of the gradient. However, any difference in the magnitude causes systematic errors in gradient components which depend on the gradient direction too. ~~It affects the gradient magnitudes, not their directions, however, the gradient direction results in different projections into gradient components. In a global scope,~~At global scale, ~~a~~ the long-term mean gradient pointing to the equator causes systematic differences up to 0.3 mm in the north gradient component between Bar-Sever and Chen and Herring *mfg* (see Appendix A).

Both smaller gradient formal errors and slightly improved height repeatability which was found to be statistically significant suggest more accurate modelling when using the Bar-Sever *mfg*. ~~It also resulted in a better agreement with NWM in terms of standard deviation which, however, could be also attributed to smaller values usually calculated from NWM data.~~ Without an accurate and independent gradient product, it is still difficult to make a strong recommendation among different *mfg*s, i.e. resulting in different absolute gradient values. In any case, we could strongly recommend to use the same *mfg* implemented in the same form whenever comparing or combining tropospheric gradients derived from different sources (GNSS, WVR or NWM). On the other hand, if tropospheric gradients are used solely for reconstructing slant total delays, different *mfg*s should provide very similar results.

Appendix A

In the upper panel of Figure ~~8~~10 the systematic difference in the derived tropospheric gradients based on ERA5 data (average over 10 years) is shown for any point on Earth's surface between tropospheric gradients estimated utilizing the BS *mfg* and tropospheric gradients estimated utilizing the CH *mfg*. Whereas there is no considerable systematic difference in the east gradient component, it reaches up to 0.3 mm in the north gradient component (positive in the northern and negative in the southern hemisphere). We note that the mean tropospheric gradients point to the equator, i.e., the north gradient component is negative in the northern hemisphere and positive in the southern hemisphere. This can be seen in the lower panel of Figure ~~8~~10, showing the mean north- and east gradient component utilizing the CH *mfg*, and can be explained by the fact that the mean zenith delays increase towards the equator. The systematic difference between these two *mfgs* is due to the fact that for the same slant total delays the magnitude of tropospheric gradients which are estimated utilizing a smaller mfg are larger than the magnitude of tropospheric gradients which are estimated utilizing a larger *mfg*. The product of the *mfg* and the tropospheric gradients, i.e., the azimuth dependent part of the tropospheric delay, remains approximately the same.

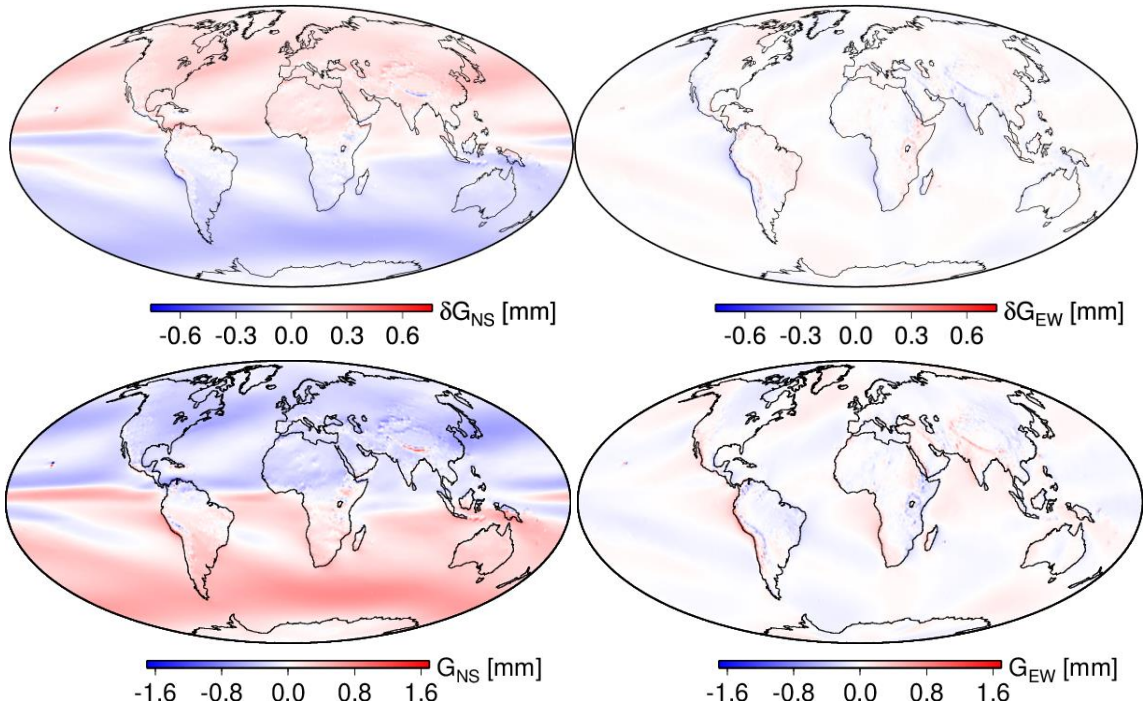

Figure ~~8~~10. Upper panel: Systematic difference (average over 10 years) for any point on Earth's surface between tropospheric gradients estimated utilizing the gradient mapping function of Bar-Sever and tropospheric gradients estimated utilizing the gradient mapping function of Chen and Herring. Lower panel: Mean north- and east gradient component (average over 10 years) for any point on Earth's surface utilizing the mapping function of Chen and Herring. Left panels show the north gradient component, right panels the east gradient component. The results are based on ERA5 data.

Appendix B

NWM tropospheric gradients presented in this paper were also compared with NWM tropospheric gradients provided by TU Vienna (see http://vmf.geo.tuwien.ac.at/). Specifically, we compared the NWM tropospheric gradients based on ERA5 with the so-called Linearized Horizontal Gradients (LHG) (Boehm et al. 2007b). We note that the LHGs are based on the closed form expression depending on the north-south and east-west horizontal gradient of refractivity (Davis et al., 1993). The LHGs are solely available for several stations, their provision ended in 2017 and they are no longer supported. Recently, Landskron and Boehm (2018) provided refined horizontal gradients based on a least square adjustment which are currently recommended to be used. We decided to look at three stations available in all data sets: ONSA, POTS and WTZR and we provide the comparisons in Figure 11. As to expect, we find a better agreement between ERA5 tropospheric gradients and the refined horizontal gradients. We also find that the magnitude of the ERA5 tropospheric gradients is larger than the magnitude of the refined horizontal gradients. This is not surprising since the NWM that is used in the generation of the refined horizontal gradients has a horizontal resolution of 1° only (ERA-Interim provided by the ECMWF). For example, Zus et al. (2016) showed how an increased horizontal resolution of the NWM amplifies the tropospheric gradient components under severe weather conditions.

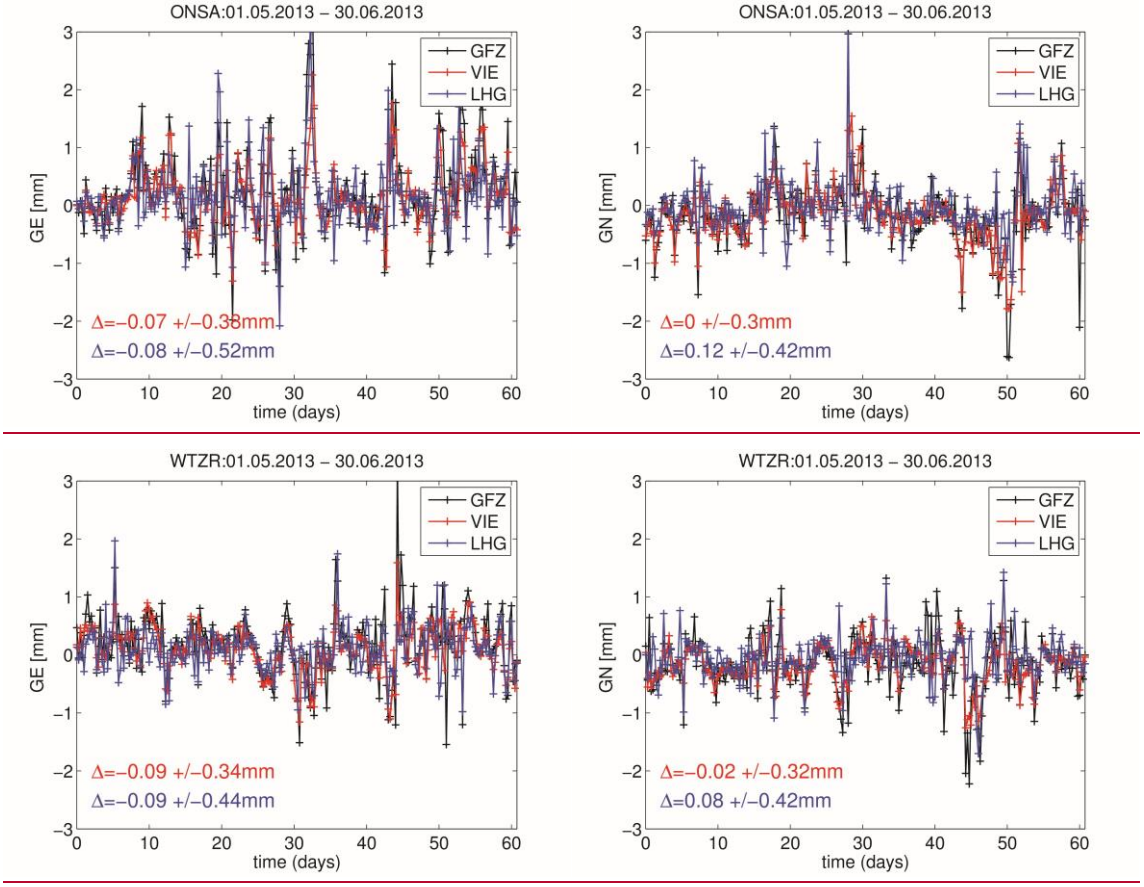

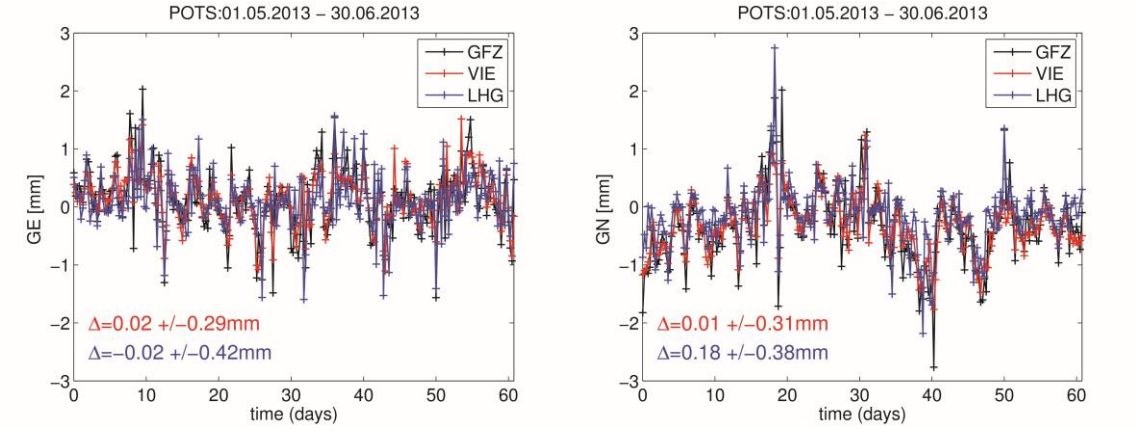

Figure 11: The left panels show the time series (May 1 – June 30, 2013) of the east-gradient component for the station ONSA, WTZR and POTS respectively. The right panels show the time series of the north-gradient component for the same stations. The black line corresponds to the ERA5 tropospheric gradients (GFZ, regarded in the paper as NWM ERA5), the red line corresponds to the refined horizontal gradients provided by TU Vienna (VIE) and the blue line corresponds to the so-called linearized horizontal gradients provided by TU Vienna (LHG). The red numbers represent the mean and standard deviation between VIE and GFZ. The blue numbers are the mean and standard deviation between LHG and GFZ.

Acknowledgement

The authors thank all the institutions which provided GNSS observations for the COST ES1206 Benchmark campaign (Douša et al., 2016). F.Z. wants to thank Dr. Thomas Schwitalla (Institute of Physics and Meteorology, University Hohenheim) for the introduction to the WRF system. The ECMWF is acknowledged for making publicly available ERA5 reanalysis fields that were generated using Copernicus Climate Change Service Information 2018 (https://www.ecmwf.int/en/forecasts/datasets/archive-datasets/reanalysis-datasets/era5). The GFS analysis fields are provided by the National Centers for Environmental Prediction (http://www.ftp.ncep.noaa.gov/data/nccf/com/gfs/prod). The study was realized during a mobility of M.K. at GFZ Potsdam funded by the EU ESIF project No. CZ.02.2.69/0.0/0.0/16_027/0008463. J.D. and P.V. acknowledge the Ministry of the Education, Youth and Science of the Czech Republic for financing the study with project No LO1506 and supporting benchmark data with project No LM2015079.

References

Ahmed, F., Václavovic, P., Teferle, F.N., Douša, J., Bingley, R. and Laurichesse, D.: Comparative analysis of real-time precise point positioning zenith total delay estimates, GPS Solutions, 20, 187, doi:10.1007/s10291-014-0427-z, 2016.

Bar-Sever, Y.E., Kroger, P.M. and Borjesson, J.A.: Estimating horizontal gradients of tropospheric path delay with a single GPS receiver. Journal of Geophysical Research, 103, B3, 5019–5035, doi:10.1029/97JB03534, 1998.

Balidakis, K., Nilsson, T., Zus, F., Glaser, S., Heinkelmann, R., Deng, Z. and Schuh, H.: Estimating Integrated Water Vapor Trends From VLBI, GPS, and Numerical Weather Models: Sensitivity to Tropospheric Parameterization, Journal of Geophysical Research: Atmospheres, 123, 6356-6372, doi: 10.1029/2017JD028049, 2018.

Bender, M., Dick, G., Ge, M., Deng, Z., Wickert, J., Kahle, H.-G., Raabe, A. and Tetzlaff, G.: Development of a GNSS water vapour tomography system using algebraic reconstruction techniques, Advances in Space Research, 47, 10, p. 1704-1720, 2011.

Bender, M., Stephan, K., Schraff, C., Reich, H., Rhodin, A. and Potthast, R.: GPS Slant Delay Assimilation for Convective Scale NWP. Fifth International Symposium on Data Assimilation (ISDA), University of Reading, UK, July 18–22, 2016.

Boehm, J., Niell, A., Tregoning, P. and Schuh, H.: Global mapping function (GMF): A new empirical mapping function based on numerical weather model data, Geophysical Research Letters, 33, 943–951, doi:10.1029/2005GL025546, 2006a.

Boehm, J., Werl, B. and Schuh, H.: Troposphere mapping functions for GPS and very long baseline interferometry from European Centre for Medium-Range Weather Forecasts operational analysis data, Journal of Geophysical Research, 111, B02406, doi:10.1029/2005JB003629, 2006b.

Boehm, J., Heinkelmann, R. and Schuh, H.: Short note: A global model of pressure and temperature for geodetic applications, Journal of Geodesy, 81, 679–683, doi:10.1007/s00190-007-0135-3, 2007a.

Boehm, J. and Schuh, H.: Troposphere gradients from the ECMWF in VLBI analysis, Journal of Geodesy, 81, 403-408, doi: 10.1007/s00190-007-0144-2, 2007b.

Brenot, H., Neméghaire, J., Delobbe, L., Clerbaux, N., Meutter, P., Deckmyn, A., Delcloo, A., Frappez, L. and Van Roozendael, M.: Preliminary signs of the initiation of deep convection by GNSS, Atmospheric Chemistry and Physics, 13, 5425–5449, doi:10.5194/acp-13-5425-2013, 2013.

Chen, G. and Herring, T. A.: Effects of atmospheric azimuthal asymmetry on the analysis of space geodetic data, Journal of Geophysical Research, 102, 20489–20502, doi:10.1029/97JB01739, 1997.

Dach, R., Lutz, S., Walser, P., and Fridez, P. (Eds.): Bernese GNSS Software Version 5.2. User manual, Astronomical Institute, University of Bern, Bern Open Publishing, 2015.

Davis, J., Elgered, G., Niell, A. and Kuehn, K.: Ground-based measurement of gradients in the “wet” radio refractivity of air, Radio Science, 28, 1003-1018, 1993.

Douša, J., Dick, G., Kačmařík, M., Brožková, R., Zus, F., Brenot, H., Stoycheva, A., Möller, G. and Kaplon, J.: Benchmark campaign and case study episode in central Europe for development and assessment of advanced GNSS tropospheric models and products, Atmospheric Measurement Techniques, 9, 2989–3008, doi:10.5194/amt-9-2989-2016, 2016.

Douša, J., Václavovic, P. and Eliaš, M.: Tropospheric products of the second European GNSS reprocessing (1996-2014), Atmospheric Measurement Techniques, 10, 3589–3607, doi:10.5194/amt-10-3589-2017, 2017.

Douša, J., Eliaš, M., Václavovic, P., Eben, K. and Krč, P. A two-stage tropospheric correction combining data from GNSS and numerical weather model, GPS Solutions, 22, 77, doi:10.1007/s10291-018-0742-x, 2018a.

Douša, J., Václavovic, P., Zhao, L. and Kačmařík, M.: New Adaptable All-in-One Strategy for Estimating Advanced Tropospheric Parameters and Using Real-Time Orbits and Clocks, Remote Sensing, 10, 232, doi:10.3390/rs10020232, 2018b.

Flores, A., Ruffini, G. and Rius, A.: 4D tropospheric tomography using GPS slant wet delays, Annales Geophysicae, 18, 223–234, doi:10.1007/s00585-000-0223-7, 2000.

Guerova, G., Bettems, J. M., Brockmann, E. and Matzler, C.: Assimilation of COST 716 Near-Real Time GPS data in the nonhydrostatic limited area model used at MeteoSwiss, Meteorol. Atmos. Phys., 91, 149–164, doi:10.1007/s00703-005-0110-6, 2006.

Guerova, G., Jones, J., Dousa, J., Dick, G., de Haan, S., Pottiaux, E., Bock, O., Pacione, R., Elgered, G., Vedel, H., and Bender, M.: Review of the state-of-the-art and future prospects of the ground-based GNSS meteorology, Atmospheric Measurement Techniques, 9, 5385-5406, doi:10.5194/amt-9-5385-2016, 2016.

Iwabuchi, T., Miyazaki, S., Heki, K., Naito, I. and Hatanaka, Y.: An impact of estimating tropospheric delay gradients on tropospheric delay estimations in the summer using the Japanese nationwide GPS array, Journal of Geophysical Research, 108, D10, 4315, doi:10.1029/2002JD002214, 2003.

Järvinen, H., Eresmaa, R., Vedel, H., Salonen, K., Niemelä, S. and de Vries, J.: A variational data assimilation system for ground-based GPS slant delays, Q. J. R. Meteorol. Soc., 133, 969–980, doi:10.1002/qj.79, 2007.

Kačmařík, M.: Retrieving of GNSS Tropospheric Delays from RTKLIB in Real-Time and Post-processing Mode, In Lecture Notes in Geoinformation and Cartography, Proceedings of GIS Ostrava 2017, Ivan, I., Horák, J., Inspektor, T., Springer, Cham, doi:10.1007/978-3-319-61297-3_13, 2018.

Kawabata, T., Shoji, Y., Seko, H. and Saito, K.: A Numerical Study on a Mesoscale Convective System over a Subtropical Island with 4D-Var Assimilation of GPS Slant Total Delays, Journal of the Meteorological Society of Japan, 91, 705–721, doi:10.2151/jmsj.2013-510, 2013.

Kouba, J.: Testing of global pressure/temperature (GPT) model and global mapping function (GMF) in GPS analyses, Journal of Geodesy, 83, 199–208, doi:10.1007/s00190-008-0229-6, 2009.

Landskron, D. and Boehm, J.: Refined discrete and empirical horizontal gradients in VLBI analysis, Journal of Geodesy, 92, 1387-1399, doi:10.1007/s00190-018-1127-1, 2018.

Li, X., Zus, F., Lu, C., Ning, T., Dick, G., Ge, M., Wickert, J. and Schuh, H.: Retrieving high-resolution tropospheric gradients from multiconstellation GNSS observations, Geophysical Research Letters, 42, 4173–4181, doi: 10.1002/2015GL063856, 2015.

Meindl, M., Schaer, S., Hugentobler, U. and Beutler, G.: Tropospheric Gradient Estimation at CODE: Results from Global Solutions, Journal of the Meteorological Society of Japan, 82, 1B, 331-338, doi:10.2151/jmsj.2004.331, 2004.

Morel, L., Pottiaux, E., Durand, F., Fund, F., Boniface, K., de Oliveira, P.S. and Van Baelen, J.: Validity and behaviour of tropospheric gradients estimated by GPS in Corsica, Advances in Space Research, 55, 135-149, doi:10.1016/j.asr.2014.10.004, 2015.

Rothacher, M. and Beutler, G.: The role of GPS in the study of global change, Physics and Chemistry of the Earth, 23, 9-10, doi:10.1016/S0079-1946(98)00143-8, 1998.

Saastamoinen, J.: Atmospheric Correction for the Troposphere and Stratosphere in Radio ranging of satellites, Geophysical Monograph Series, 15, 247–251, doi:10.1029/gm015p0247, 1972.

Shoji, Y., Kunii, M. and Saito, K.: Assimilation of Nationwide and Global GPS PWV Data for a Heavy Rain Event on 28 July 2008 in Hokuriku and Kinki, Japan. Scientific Online Letters on the Atmosphere, 5, 45–48, doi:10.2151/sola.2009-012, 2009.

Skamarock, W.C., Klemp, J.B., Dudhia, J., Gill, D.O., Barker, D.M., Duda, M.G., Huang, X.Y., Wang, W. and Powers, J.G.: A description of the advanced research WRF version 3. NCAR tech. note NCAR/TN-475+STR, doi:10.5065/D68S4MVH, 2008.

Václavovic, P., Douša, J. and Györi, G.: G-Nut software library - State of development and first results, Acta Geodynamica et Geomaterialia, 10, 4, 431-436, doi:10.13168/AGG.2013.0042, 2014.

Václavovic, P. and Douša, J.: Backward smoothing for precise GNSS applications, Advances in Space Research, 56, 8, 1627-1634, doi:10.1016/j.asr.2015.07.020, 2015.

Vedel, H. and Huang, X.: Impact of Ground Based GPS Data on Numerical Weather Prediction, Journal of the Meteorological Society of Japan, 82, 459–472, doi:10.2151/jmsj.2004.459, 2004.

Walpersdorf, A., E. Calais, J. Haase, L. Eymard, M. Desbois and H. Vedel, Atmospheric gradients estimated by GPS compared to a high resolution numerical weather prediction (NWP) model, Physics and Chemistry of the Earth, Part A: Solid Earth and Geodesy, 26 (3), 147-152, doi:10.1016/S1464-1895(01)00038-2, 2002.

Zhou, F., Li, X., Li, W., Chen, W., Dong, D., Wickert, J. and Schuh, H.: The Impact of Estimating High-Resolution Tropospheric Gradients on Multi-GNSS Precise Positioning, Sensors, 17, 756, doi:10.3390/s17040756, 2017.

Zumberge, J. F., Heflin, M. B., Jefferson, D. C., Watkins, M. M. and Webb, F. H.: Precise point positioning for the efficient and robust analysis of GPS data from large networks, Journal of Geophysical Research, 102, 5005–5017, doi:10.1029/96JB03860, 1997.

Zus, F., Bender, M., Deng, Z., Dick, G., Heise, S., Shang-Guan, M. and Wickert, J.: A methodology to compute GPS slant total delays in a numerical weather model, Radio Science, 47, RS2018, doi:10.1029/2011RS004853, 2012.

Zus, F., Dick, G., Heise, S. and Wickert, J.: A forward operator and its adjoint for GPS slant total delays, Radio Science, 50, 393–405, doi: 10.1002/2014RS005584, 2015.

Zus, F., Douša, J., Dick., G. and Wickert, J.: Station specific NWM based tropo parameters for the Benchmark campaign, ES1206-GNSS4WEC COST Workshop, Iceland, 8–10 March 2016.

Zus, F., Douša, J., Kačmařík, M., Václavovic, P., Dick, G. and Wickert, J.: Estimating the Impact of Global Navigation Satellite System Horizontal Delay Gradients in Variational Data Assimilation, Remote Sensing, 11, 41, doi:10.3390/rs11010041, 2019.